Sensitivity and identifiability analysis for a model of the propagation and control of COVID-19 in Chile

Raimund Bürger · Gerardo Chowell · Ilja Kröker · Leidy Yissedt Lara-Díaz

February 17, 2021

Abstract A compartmental model is formulated to describe the progression of the COVID-19 pandemic in Chile, where each of the 16 administrative regions is considered as a separate population. Parameters of this model, and in particular the basic reproductive number R_0, can be estimated by fitting the model to published information on the progression of the epidemic in each region. The adjustment of appropriate model parameters can be achieved by either the Simulated Annealing (SA) method or alternatively, by a stochastic optimization model using a classical Markov chain Monte Carlo (MCMC) technique. This estimation allows one to analyze the identifiability and sensitivity of the parameters. The approach considers the control policies applied in Chile for mitigating the outbreak of COVID-19, in particular the methodology assumed by the government to declare the quarantine measures. The outbreaks are followed in a regional scale taking into account the different dates of the first case, the quarantine measures adapted to the regional situation, and the different criteria applied to the selection of data.

Keywords COVID-19 model · dynamical quarantines · parameter estimation · sensitivity indices · basic reproductive number · simulated annealing · Markov chain Monte Carlo method

R. Bürger, L.Y. Lara-Díaz
CI^{2}MA and Departamento de Ingeniería Matemática, Facultad de Ciencias Físicas y Matemáticas, Universidad de Concepción, Casilla 160-C, Concepción, Chile.
E-mail: rburger@ing-mat.udec.cl, E-mail: llara@ing-mat.udec.cl

G. Chowell
School of Public Health, Georgia State University, Atlanta, Georgia, USA
Simon A. Levin Mathematical and Computational Modeling Sciences Center, School of Human Evolution and Social Change, Arizona State University, Tempe, AZ 85287, USA
Division of International Epidemiology and Population Studies, Fogarty International Center, National Institute of Health, Bethesda, MD 20892, USA
E-mail: gchowell@gsu.edu

I. Kröker
Stochastic Simulation & Safety Research for Hydrosystems (LS3),
Institute for Modelling Hydraulic and Environmental Systems (IWS),
Universität Stuttgart, Pfaffenwaldring 5a, D-70569 Stuttgart, Germany
E-mail: ilja.kroeker@iws.uni-stuttgart.de

1 Introduction

1.1 Scope

The COVID-19 pandemic is currently the main topic of daily news worldwide. We recall that the coronavirus disease 2019 (COVID-19), caused by severe acute respiratory syndrome coronavirus 2 (SARS-CoV-2), was declared a global pandemic by the World Health Organization (WHO) on March 11, 2020 [1, 2]. This highly contagious unprecedented virus has impacted government and public institutions, strained the health care systems, restricted people in their homes, and caused country-wide lockdowns resulting in a global economic crisis [3–5]. The impact of COVID-19 at the time of writing of this paper (February 15, 2021) amounts to roughly 109 million cases and 2.4 million deaths worldwide.

The morbidity, mortality, and economic indicators associated with the COVID-19 pandemic point to a devastating picture for Latin American countries. High poverty rates, poor leadership, high prevalence of underlying health conditions such as obesity and diabetes, and frail healthcare systems have exacerbated the impact of the novel coronavirus in this region [6–9]. In Chile, the Ministry of Health reported the first COVID-19 case on March 3, 2020, becoming the fifth country in Latin America after Brazil, Mexico, Ecuador and Argentina to report COVID-19 cases. Soon after, the Chilean government put in place a number of interventions including the closure of all daycares, schools, and universities (March 16), border controls, telework recommendations (March 18), closure of non-essential businesses (March 19), national night curfews (March 22), as well as targeted lockdowns at the level of municipalities since March 26, 2020. As of February 15, 2021, Chile has accumulated a total of 779541 cases and 19624 deaths [10]. It is also worth noting that Chile has tested at a higher rate than any other Latin American country [11]. Fortunately, Chile has started a mass COVID-19 vaccination campaign with the goal of immunizing about 80% of the population by June 2021 (see, for instance, [12]).

It is the purpose of this contribution to advance a compartmental model of the progression of COVID-19 in Chile, where each of the 16 administrative regions is considered as a separate population. It is demonstrated how parameters of this model, and in particular the basic reproductive number R_0, can be estimated from the model by utilizing published information on the progression of the epidemic in each region. The adjustment of appropriate model parameters can be achieved by either the Simulated Annealing (SA) method or alternatively, by a stochastic optimization model using a classical Markov chain Monte Carlo (MCMC) technique. The parameter estimation allows us to address problems of parameter identifiability and sensitivity of R_0 in each region with respect to the model parameters. Our study covers the early transmission dynamics in Chile, considering the period from early March 2020 to July 27, 2020. (On July 28, 2020, a new, and to date quite successful step-by-step system of county-wise levels of quarantine was introduced. This measure would require a new definition of quarantine, so we chose July 27, 2020 as the end of our time interval of coverage.)

1.2 Related work

To put the paper into the proper perspective, we first recall that introductions to compartmental epidemiological models are provided in [13–18]. This class of models goes back to the well-known work of Kermack and McKendrick [19]. Within a compartmental model the total population is subdivided into at least two epidemiological compartments (say, susceptible and infected; but many others can be considered). The rates of progression between the compartments, as well as the incidence and possibly birth and death of individuals, need to be specified, which leads to a system of coupled, and mostly nonlinear ordinary differential equations (ODEs) that describe the progression of the epidemic. The compartmental approach makes predictions on the basic reproductive number R_0 that gives the number of secondary cases one infectious individual will produce in a population consisting only of susceptible individuals [17, p. 21]. A simpler class of models are so-called phenomenological growth models (PGMs) that describe the evolution of the total size of the epidemic (the cumulative number of cases). Such models only require a small number of parameters are commonly used to describe epidemic growth patterns, and can be expressed by a scalar ODE that in many cases can even be solved in closed form (see [20–26] and the literature cited in these works).

The identification of parameters included in a compartmental model, and whose combination (depending on the model) eventually provides R_0, requires comparing the simulated time-dependent progression of the epidemic, that is simulations of the evolution of the different epidemic compartments, with (observed) datasets of the same quantities. One then tries to minimize, in a sense to be made precise, the difference between the simulated and observed data in order to obtain the parameters that characterize a specific epidemic outbreak in a determined region. The same task persists for PGMs. Among the methodologies available for parameter identification we choose herein SA method and an alternative method based on an MCMC technique with the Metropolis-Hastings algorithm [27, 28]. References to the SA and MCMC methods include [29–32] and [33–37], respectively.

Specifically with respect to COVID-19, we mention that the outbreak of the pandemic was almost immediately followed by efforts to model its evolution mathematically globally, at the level of whole countries, or in communities (say, individual counties) and regions of small spatial scale. The broad aim of these studies is to estimate the transmission potential of COVID-19, and of course to devise and evaluate appropriate control strategies such as quarantines, social distancing, use of personal protective equipment (PPE; such as wearing masks in public, handwashing, etc.), and vaccination. Among the studies that are consistent with our approach we mention that compartmental models have been proposed to describe the transmission of the pandemic in China [39, 40], Brazil [41], India [42], and Spain [43], as well as PGMs applied to the pandemic situation in Chile [44] and Mexico [45].

Finally, we mention that the present work does not include mobility between regions. In principle, our approach treats the populations of all regions independently following Chowell et al. [38] in combination with [39] (for the case of China). An improvement of the model predictive quality could be achieved by explicitly incorporating human mobility between regions, especially for early stages of an epidemic that pre-date travel restrictions. The incorporation of inter-regional mo-

bility within a metapopulation approach is described, for instance, in [43, 46–50]. For the special case of Chile, a model of travel between regions within a metapopulation model describing the progression of the 2009 A/H1N1 influenza pandemic was introduced in [51].

1.3 Outline of the paper

The remainder of this paper is organized as follows. The compartmental model for a single population, which is a based on [38] combined with the description of quarantines of [39], is introduced in Section 2, starting with a description of compartments and transmission rates (Section 2.1). Then, by using the next-generation matrix approach, we derive in Section 2.2 basic and effective reproduction numbers (R_0 and $R(t)$) for the model in terms of the parameters. Next, in Section 3 we describe the early transmission dynamics of COVID-19 in Chile, including some basic information on geography and population as well as early policies to control the pandemic (see Section 3.1) followed by an overview of representative values of the parameters of the compartmental model (Section 3.2). In fact, some of these parameters have fixed values depending on the spread of the SARS-CoV-2 virus while others depend on the region under study, and yet others will be estimated using the Chilean data. Section 4 describes the procedure of estimating the two latter classes of parameters. To this end, we first specify in Section 4.1 two parameters, namely the transmission rate and the proportion of fully infectious individuals who undergo testing, as time-dependent functions. Then, in Section 4.2, we outline the mentioned SA and MCMC techniques within our context. As we briefly discuss in Section 5, both techniques can be utilized to calculate confidence intervals for the parameters identified. Roughly speaking, the smallness of a confidence interval indicates that the corresponding parameter can well be identified. Another issue related to parameter identification is the analysis of sensitivity of the basic reproductive number R_0 with respect to the different parameters, that is, one wishes to quantify the relative change in R_0 when a parameter changes. This approach is outlined in Section 6. Section 7 is dedicated to the presentation of the results of applying the methods of Sections 4 to 6 to the data of the COVID-19 outbreak in Chile introduced in Section 3. We address the results on parameter identification, identifiability analysis, and sensitivity analysis in Sections 7.1, 7.2, and 7.3 respectively. In particular we compare results obtained by the alternative SA and MCMC methodologies. Finally, some conclusions are collected in Section 8. An appendix contains tables of results pertaining to Section 7.

2 Mathematical model

2.1 Compartments and transmission rates

In what follows, we consider a single population and adopt a simplified version of the model by Chowell et al. [38], combined with the way individuals in quarantine are described in [39]. Individuals within the model are classified as susceptible (S), in home quarantine (Q), latent (E_1), partially infectious but not yet symptomatic (E_2), asymptomatic (A), infectious and will not be tested (I_n), infectious and will

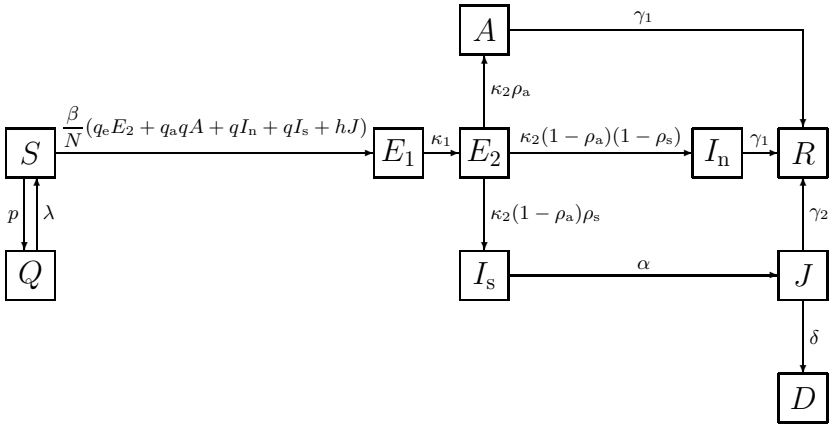

Fig. 1 Schematic of the transmission of COVID-19 for one population

Table 1 Description of parameters

Parameter	Description
β	transmission rate
h	relative isolation transmissibility of infected individuals
q_e	relative transmissibility of exposed individuals
q_a	relative transmissibility of asymptomatic cases
q	level of effectiveness of PPE such as mask and wand washing
$1/\kappa_1$	length of latent period
$1/\kappa_2$	length of infectiousness prior to symptom onset
ρ_a	proportion of exposed individuals who become asymptomatically infected
ρ_s	proportion of fully infectious individuals who undergo testing
$1/\alpha$	time from symptom onset to isolation or hospitalization
$1/\gamma_1$	time from illness onset to recovery
$1/\gamma_2$	time from diagnosis to recovery
δ	death rate within hospitals
p	proportion of the susceptible population in quarantine declared
$1/\lambda$	duration of quarantine

be tested and isolated (I_s), hospitalized/isolated infectious (J), recovered (R), and deceased (D). Constant population size is assumed, i.e.,

$$N := S + Q + E_1 + E_2 + A + I_n + I_s + J + R + D = \text{const.} \tag{1}$$

Note that we stipulate one single class of asymptomatic individuals, while in [38] a distinction is made between individuals that are "asymptomatic and will not be tested" and those that are "asymptomatic and will be tested and will be isolated".

For the home-quarantined individuals it is assumed that due to severe travel restrictions and rigorous supervision by their local communities, they do not have contact with infected individuals. The parameters p and λ represent the percentage of individuals in quarantine and the quarantine duration, respectively. Therefore, if $p = \lambda = 0$ there is no quarantine and the class Q has the effect of removing susceptible individuals from the infection dynamics.

Five classes can contribute to new infections, namely E_2, A, I_n, I_s, and J. If we denote by $r_{X\to Y}$ the rate at which individuals move from class X to class Y,

then susceptible individuals move to E_1 at rate

$$r_{S\to E_1} = \frac{\beta}{N}(q_{\mathrm{e}}E_2 + q_{\mathrm{a}}qA + qI_{\mathrm{n}} + qI_{\mathrm{s}} + hJ),$$

where β denotes the overall transmission rate. Individuals in E_1 progress to E_2 at rate κ_1. Individuals from E_2 are partially infectious, with relative transmissibility q_{e}, and progress at rate κ_2, where a proportion ρ_{a} become asymptomatic and partially infectious (relative transmissibility q_{a}), and $1-\rho_{\mathrm{a}}$ become fully infectious. Among the proportion $1-\rho_{\mathrm{a}}$ that become fully infectious, ρ_{s} will be tested, while $1-\rho_{\mathrm{s}}$ will be undetected. Asymptomatic individuals who are not tested and symptomatic individuals wear personal protective equipment (PPE) (such as wearing masks in public, handwashing, etc.) and thus have relative transmissibility q, which is proportional to the level of effectiveness of PPE. Individuals within classes A and I_{n} (who are not tested) recover at rate γ_1. Those who are tested (class I_{s}) will progress to the hospitalized and isolated class at diagnosis rate α. Relative transmission within hospitals and isolated places may occur, but we assume perfect isolation in our analysis. Individuals who are hospitalized and isolated progress to the recovered class at rate γ_2 or to the deceased class at rate δ. Therefore, the model is defined by the following system of non-linear differential equations for a single population, where all variables in capital letters are functions of time t, i.e. it is understood that $S = S(t)$, $E_1 = E_1(t)$, etc., and a prime denotes the derivative, that is $S' \equiv \mathrm{d}S/\mathrm{d}t$, etc. The auxiliary variable C tracks the cumulative number of diagnosed/reported cases from the start of the outbreak, and C' represents the new diagnosed cases.

$$S' = -\frac{\beta S}{N}(q_{\mathrm{e}}E_2 + q_{\mathrm{a}}qA + qI_{\mathrm{n}} + qI_{\mathrm{s}} + hJ) - pS + \lambda Q, \tag{2a}$$
$$Q' = pS - \lambda Q, \tag{2b}$$
$$E_1' = \frac{\beta S}{N}(q_{\mathrm{e}}E_2 + q_{\mathrm{a}}qA + qI_{\mathrm{n}} + qI_{\mathrm{s}} + hJ) - \kappa_1 E_1, \tag{2c}$$
$$E_2' = \kappa_1 E_1 - \kappa_2 E_2, \tag{2d}$$
$$A' = \kappa_2 \rho_{\mathrm{a}} E_2 - \gamma_1 A, \tag{2e}$$
$$I_{\mathrm{n}}' = \kappa_2(1-\rho_{\mathrm{a}})(1-\rho_{\mathrm{s}})E_2 - \gamma_1 I_{\mathrm{n}}, \tag{2f}$$
$$I_{\mathrm{s}}' = \kappa_2(1-\rho_{\mathrm{a}})\rho_{\mathrm{s}} E_2 - \alpha I_{\mathrm{s}}, \tag{2g}$$
$$J' = \alpha I_{\mathrm{s}} - (\gamma_2 + \delta)J, \tag{2h}$$
$$R' = \gamma_1(A + I_{\mathrm{n}}) + \gamma_2 J, \tag{2i}$$
$$D' = \delta J, \tag{2j}$$
$$C' = \alpha I_{\mathrm{s}}. \tag{2k}$$

A schematic of the transmissions is provided in Figure 1, and the description of the parameters is given in Table 1.

2.2 Reproduction numbers

The basic and effective reproduction numbers R_0 and R are quantities that allow us to measure the epidemic impact of infectious disease in a population as well as

measuring the effectiveness of control measures. The basic reproduction number R_0 defines the average number of secondary cases generated by primary infectious individuals during the early transmission, this is when the population is completely susceptible and in the absence of control interventions. And effective reproduction number R is defined to partially susceptible population, where if $R > 1$, the infection can be transmitted within the population, and if $R < 1$ the infection cannot spread. To calculate these numbers, we use the next-generation matrix approach [52]. This yields the expression

$$\begin{aligned} R_0 &= \rho(\boldsymbol{\mathcal{F}}\boldsymbol{\mathcal{V}}^{-1}) \\ &= \beta\left(\frac{q_{\mathrm{e}}}{\kappa_2} + \frac{q_{\mathrm{a}}q\rho_{\mathrm{a}}}{\gamma_1} + \frac{q(1-\rho_{\mathrm{s}})(1-\rho_{\mathrm{a}})}{\gamma_1} + \frac{q\rho_{\mathrm{s}}(1-\rho_{\mathrm{a}})}{\alpha} + \frac{h\rho_{\mathrm{s}}(1-\rho_{\mathrm{a}})}{\gamma_2+\delta}\right), \end{aligned} \tag{3}$$

where ρ denotes the spectral radius and the matrices $\boldsymbol{\mathcal{F}}$ and $\boldsymbol{\mathcal{V}}$ are given by the respective expressions

$$\boldsymbol{\mathcal{F}} = \begin{bmatrix} 0 & \beta q_{\mathrm{e}} & \beta q_{\mathrm{a}} q & \beta q & \beta q & \beta h \\ 0 & 0 & 0 & 0 & 0 & 0 \\ 0 & 0 & 0 & 0 & 0 & 0 \\ 0 & 0 & 0 & 0 & 0 & 0 \\ 0 & 0 & 0 & 0 & 0 & 0 \end{bmatrix},$$

$$\boldsymbol{\mathcal{V}} = \begin{bmatrix} \kappa_1 & 0 & 0 & 0 & 0 & 0 \\ -\kappa_1 & \kappa_2 & 0 & 0 & 0 & 0 \\ 0 & -\kappa_2\rho_{\mathrm{a}} & \gamma_1 & 0 & 0 & 0 \\ 0 & -\kappa_2(1-\rho_{\mathrm{a}})(1-\rho_{\mathrm{s}}) & 0 & \gamma_1 & 0 & 0 \\ 0 & -\kappa_2(1-\rho_{\mathrm{a}})\rho_{\mathrm{s}} & 0 & 0 & \alpha & 0 \\ 0 & 0 & 0 & 0 & -\alpha & \gamma_2+\delta \end{bmatrix}.$$

Moreover, the corresponding effective reproduction number is defined as

$$R(t) = R_0 S(t)/N, \tag{4}$$

where $S(t)/N$ is the proportion of susceptible individuals in the population at time t and we recall that the total population N is assumed to be constant (see (1)). From the explicit expression (3) we can deduce the following contributions of the individual compartments:

$$\begin{aligned} R^{E_2} &= \frac{\beta q_{\mathrm{e}}}{\kappa_2}, \quad R^{A} = \frac{\beta q_{\mathrm{a}} q \rho_{\mathrm{a}}}{\gamma_1}, \quad R^{I_{\mathrm{n}}} = \frac{\beta q(1-\rho_{\mathrm{s}})(1-\rho_{\mathrm{a}})}{\gamma_1}, \\ R^{I_{\mathrm{s}}} &= \frac{\beta q \rho_{\mathrm{s}}(1-\rho_{\mathrm{a}})}{\alpha}, \quad R^{J} = \frac{\beta h \rho_{\mathrm{s}}(1-\rho_{\mathrm{a}})}{\gamma_2+\delta}, \end{aligned}$$

where

$$R_0 = R^{E_2} + R^{A} + R^{I_{\mathrm{n}}} + R^{I_{\mathrm{s}}} + R^{J}. \tag{5}$$

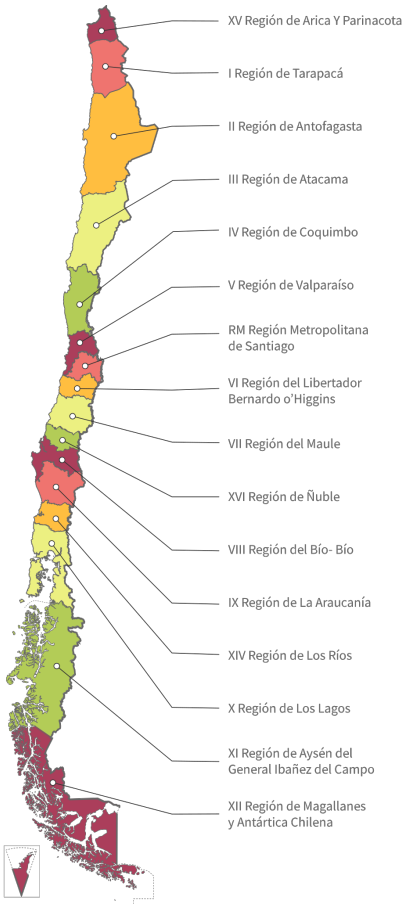

Number	Region	population
15	Arica	226.068
1	Tarapacá	330.558
2	Antofagasta	607.534
3	Atacama	286.168
4	Coquimbo	757.586
5	Valparaíso	1.815.902
6	O'Higgins	914.555
7	Maule	1.044.950
16	Ñuble	480.609
8	Biobío	1.556.805
9	Araucanía	957.224
14	Los Ríos	384.837
10	Los Lagos	828.708
11	Aysén	103.158
12	Magallanes	166.533
13	Metropolitana	7.112.808
total		17.574.003

Fig. 2 The 16 administrative regions of Chile [53] and their population according to the 2017 census [54]. The Roman numbers are the official administrative numbers of the geographic regions. The greater Santiago area is the Metropolitan region (RM) and counted as region 13. Note that numbering is not strictly ordered from north to south; regions 14 to 16 have been created by dividing existing regions. The total population at the end of 2020 is estimated at 19.1 million.

3 The early transmission of COVID-19 in Chile

3.1 General remarks on the early stages of COVID-19 in Chile

We wish to apply the COVID-19 model of Section 2 to each of the 16 administrative regions of Chile (see Figure 2), where each region was subject to different quarantine periods, a situation the government named "dynamical quarantines". This policy was in effect until July 27, 2020. In addition, this measure was applied only to municipalities with a greater incidence of positive cases for COVID-19. For this reason we consider a decoupled analysis for regions until July 27, 2020, assuming the day of the first positive case as the first day for the timeline of each region, and July 27, 2020 as the last day. Since the onset of the outbreak of COVID-19

Table 2 Strategies applied to attack the Covid-19 emergency in Chile

Date	Measure
16 Mar	Closing of schools and universities
18 Mar	Declaration of national emergency and border closure
19 Mar	Store closings except for pharmacies, banks, and supermarkets
21 Mar	Closing of entertainment centers
22 Mar	Declaration of national curfew between 10:00 PM and 5:00 AM
26 Mar	Start of lockdown and quarantine in different municipalities
8 Apr	Mandatory use of face masks in public spaces
25 Jul	Declaration of the new action plan named "Paso a Paso" where the different municipalities will assume a risk level (between five) according to some epidemiological criteria, with which these would have more mobility flexibilities or more restrictions.

Table 3 Changes in criteria of reported data

Date	New criterion
29 Apr	Incorporation to the number of infectious reported, to individuals with and without symptoms and with PCR positive.
1 Jun	Announcement of a new criterion, where are incorporated deaths without a diagnosis but with suspicion of COVID-19, for they have symptoms or PCR indeterminate.
2 Jun	Stop reporting the number of PCR tests for each region (for some days).
3 Jun	Stop reporting the recovered cases.
7 Jun	653 deaths are added as possible cases of COVID-19 and 96 new deaths of the people diagnosed, but the distribution of these deaths for each region is not clear, due to an update in the residence address of the deceased, where some change region
17 Jun	31422 cases are added to data because these were not notifying in the system, for this reason they are incorporated with status "without notifying" in the daily reports.

in Chile, the Ministry of Health has been reporting daily new cases of infection and death for each region and new cases of recovered persons at national level. These two last pieces of information formed a topic debate because the ministry changed the criteria for the count of deaths and used a formula for determining the recovered population based on assuming the recovery period of 14 days (see [55, 56] for official information). On information reported we also have access to the daily numbers of polymerase chain reaction (PCR) tests applied, as well as the daily number of critical patients and UCIs. Moreover, we have a timeline of strategies and measures implemented to attack the emergency that is summarized in Table 2.

At several dates the Chilean Ministry of Health changed some of the criteria to count infectious and death cases. Some moments have stopped the publication of the number of PCR for each region and recovery national cases. Table 3 indicates some of these changes along with their dates. Using the data available and taking into account the difficulties that the changes of criteria imply, we do not consider deaths data as data for our model. Still, we consider data reported as the symptomatic and asymptomatic cases, since the latter may become symptomatic later. In some cases, we also added the cases without notifying which are reported

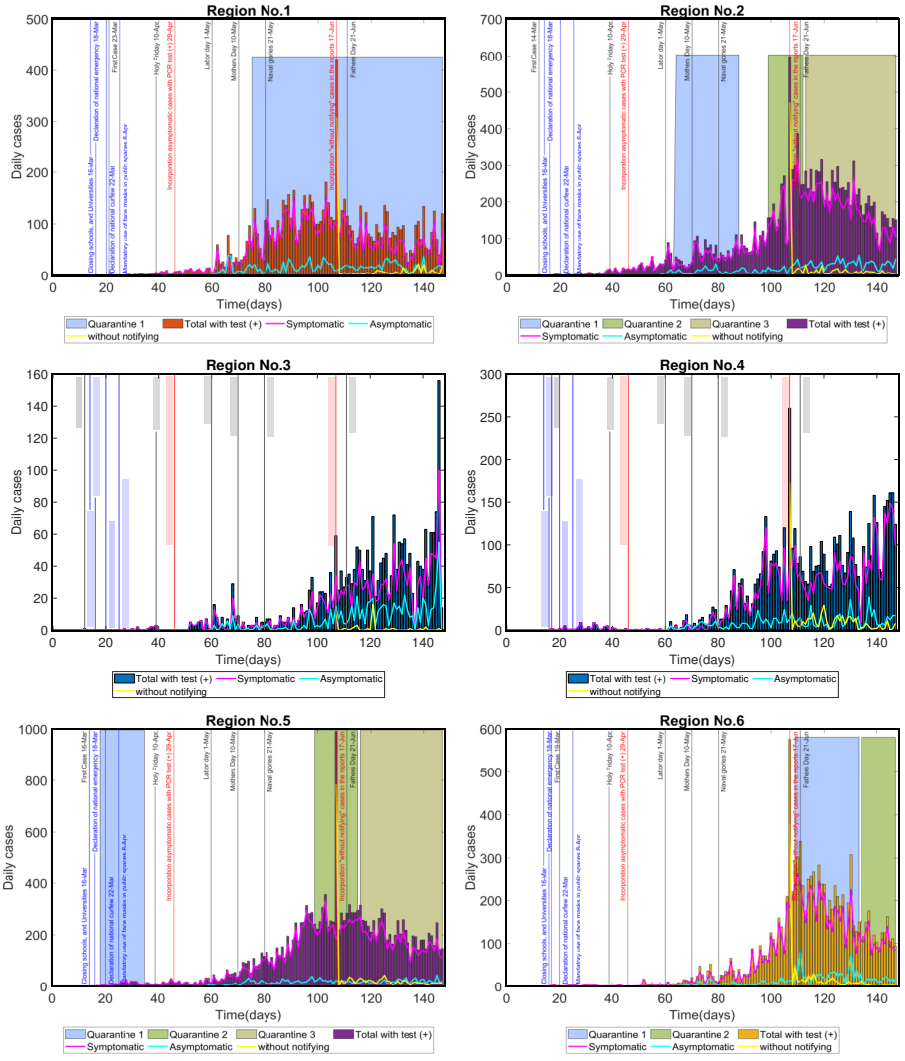

Fig. 3 Daily data at regional level (regions 1 to 6).

late. Figures 3, 4 and 5 display the different regional data distributions, including some dates of quarantine measures and important holidays.

3.2 Parameter information

Some of the parameters involved in our model have fixed values depending on the spread of the SARS-CoV-2 virus while those of others depend on the region under study or will be estimated using the Chilean data. The methodology for this last part will be exposed with more detail in the next section. The aim is to study the spread of COVID-19 and the quarantine measures applied in each

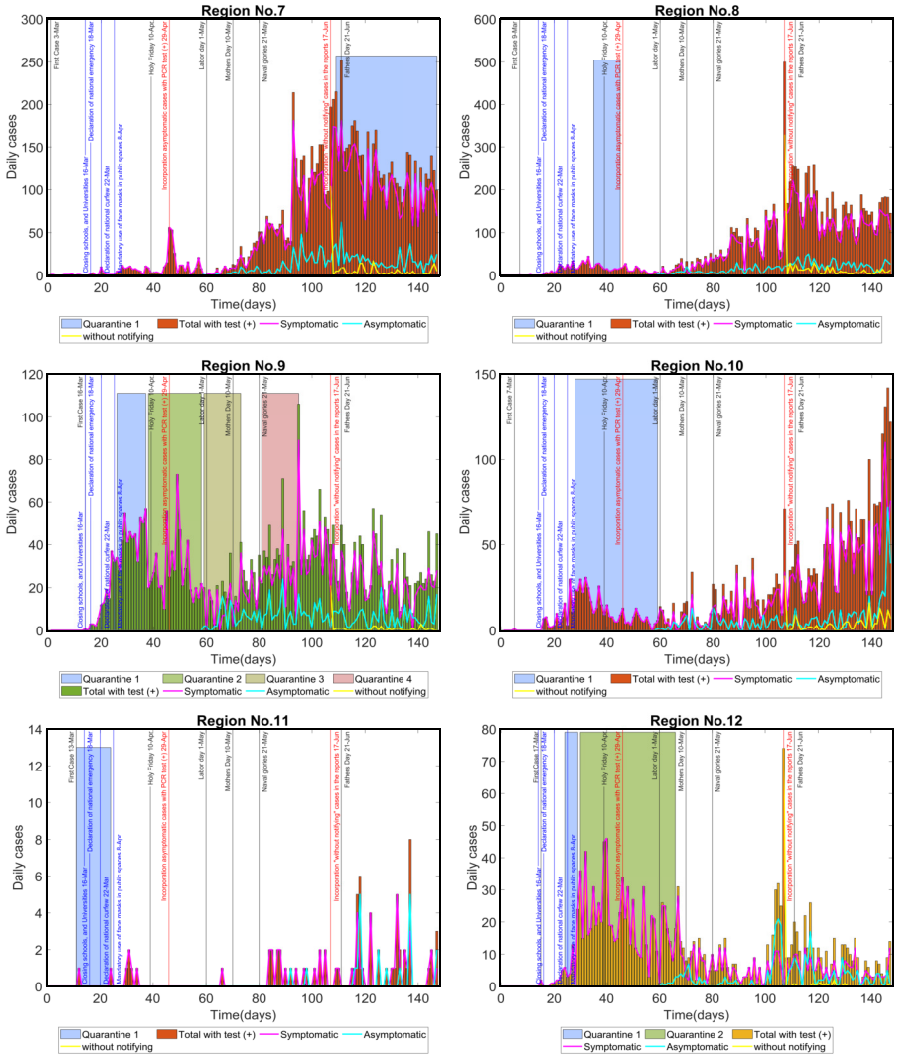

Fig. 4 Daily data at regional level (regions 7 to 12).

Chilean region (decoupled analysis). Table 5 collects the parameters along with their values, ranges, and sources, where for simplicity we assume $h = 0$, and the parameters that depend on the spread of the SARS-CoV-2 virus, namely κ_1, κ_2, γ_1, γ_2, ρ_a, q_a and q_e are collected from various references.

The quarantine parameters λ and p are determined for each region through the different quarantines declared. D ue to the increasing positive cases of COVID-19 and the increased death, control measures were applied in each region depending on the health crisis level. For example, the Metropolitan region (region 13) implemented various changes on the quarantine measure, where included or removed population of different municipalities from the Chilean region, these changes were applied for day and other for each week. The rigorous information about these

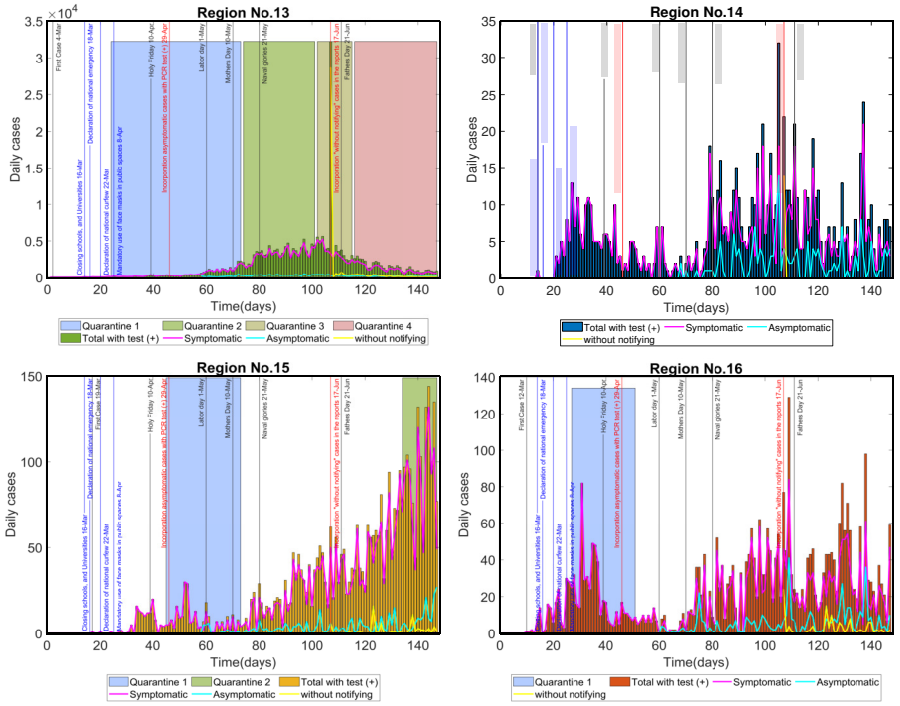

Fig. 5 Daily data at regional level (regions 13 to 16).

Table 4 Summary of the quarantine periods applied for each region. The dates correspond to a new quarantine period applied to a proportion different from the regional population.

Cod	Region	Quarantine 1	Quarantine 2	Quarantine 3	Quarantine 4	Quarantine 5	Quarantine 6
15	Arica	16 Apr–14 May	14–27 Jul				
1	Tarapacá	16 May–11 Jun	12 Jun–27 Jul				
2	Antofagasta	5–29 May	9–22 Jun	23 Jun–27 Jul			
5	Valparaíso	20 Mar–6 Apr	9–11 Jun	12–18 Jun	19–25 Jun	26 Jun–27 Jul	
6	O'Higgins	19–25 Jun	26 Jun–13 Jul	14–27 Jul			
7	Maule	19 Jun–27 Jul	19 Jun–27 Jul				
16	Ñuble	29 Mar–22 Apr					
8	Biobío	6–16 Apr					
9	Araucanía	28 Mar–8 Apr	9–16 Apr	17–29 Apr	30 Apr	1–14 May	22 May–5 Jun
10	Los Lagos	30 Mar–30 Apr					
11	Aysén	13–26 Mar					
12	Magallanes	26–31 Mar	1–6 Apr	7 Apr–7 May			
13	Metropolitana	Quarantine 1 26 Mar–2 Apr	Quarantine 2 3–8 Apr	Quarantine 3 9–13 Apr	Quarantine 4 14–15 Apr	Quarantine 5 16 Apr	Quarantine 6 23–29 Apr
		Quarantine 7 17–22 Apr	Quarantine 8 30 Apr–4 May	Quarantine 9 5–7 May	Quarantine 10 8–14 May	Quarantine 11 15 May–11 Jun	Quarantine 12 12–25 Jun
		Quarantine 13 26 Jun–27 Jul					

measures at regional level is summarized in Table 4. For simplicity, we selected the dates and periods for which the control measure was in effect in such a way that the proportion of population involved remains approximately constant, i.e., the periods presented in Table 6 and Figures 3, 4, and 5 are fixed for an amount of population approximation involved with the quarantine measure, considering for both cases as last date July 27, 2020.

Table 5 Parameters, ranges, values and references assumed in our study

Parameter	Value/Range	Selected for simulations	Source
β	0-5	Estimated	
h	0	0	Assumed
q_e	0.1	0.1	57
q_a	0.4	0.4	57
q	0-100%	0.5	Assumed
$1/\kappa_1$	2.5	2.5	40, 58
$1/\kappa_2$	2.5	2.5	59, 60
ρ_a	20%, 40%, 60%	0.4	61, 62
ρ_s	0-100%	Estimated	
$1/\alpha$	12 hrs - 10 days	Estimated	
$1/\gamma_1$	7 days	7	40, 64
$1/\gamma_2$	5 days	5	65
δ	0.021 (Chilean)	0.021	National death case data
$1/\lambda$	region-specific	cf. Table 8	66
p	0-100%	Estimated	

An important point about the quarantines applied in Chilean regions is that they have special peculiarities; for example, the different quarantine periods applied to regions 2, 5, 13, 6, and 12 (in north-south ordering) established consecutively are understood as a measure of reinforcement, i.e., the period Quarantine_3, involves more population than Quarantine_2, and the case of region 9 also with consecutive quarantines but of relaxation, i.e., for each new quarantine period declared, less population is involved. The rest of the quarantine periods involve only one period or discrete times of application. For example, region 11 has only one single quarantine, but this was applied as a preventative measure, as is also the first quarantine applied to region 5, which is a discrete measure with the subsequent quarantines.

On April 29, 2020, a new criterion was applied to count the new cases, where symptomatic and asymptomatic patients with positive PCR test result are counted. Due to this fact the number of tests from April 29 on is higher than in previous days. We will assume this situation to select the parameter ρ_s. In the next section, where we intend to estimate this parameter, assuming a new definition that is presented in the section 4. Finally, the parameter q is assumed, the parameter δ is calculated using the national data from Chile for the death cases (due to or with suspicion of COVID-19) and for the positive cases for COVID-19. Then we calculate δ assuming an average between number of deaths for day t and total cases occurred at date $t-10$, considering 10 days is the mean time between contagion and death. The parameters β and α are also estimated, as will be presented in the next section.

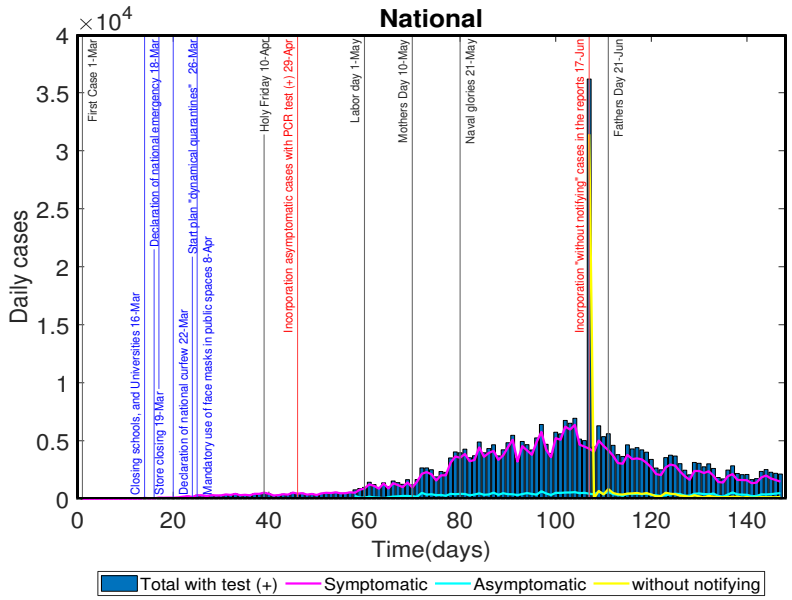

Fig. 6 Daily data at national level where the magenta, cyan, and yellow curves correspond to symptomatic, asymptomatic, and without notifying cases, respectively, the bars correspond to the total positive COVID-19 cases, that is symptomatic plus asymptomatic plus without-notifying, and vertical lines indicate important holidays and dates

Table 6 Summary of the quarantine periods applied for each region. The dates correspond to quarantine periods that approximately maintain the same proportion of the regional population.

Code	Region	Quarantine_1	Quarantine_2	Quarantine_3	Quarantine_4
15	Arica	16 Apr–14 May	14 July–27 July		
1	Tarapacá	16 May–27 Jul			
2	Antofagasta	05 May–29 May	09 Jun–22 Jun	23 Jun–27 Jul	
5	Valparaiso	20 Mar–06 Apr	09 Jun–25 Jun	26 Jun–27 Jul	
13	Metropolitana	26 Mar–14 May	15 May–11 Jun	12 Jun–25 Jun	26 Jun–27 Jul
6	O'Higgins	19 Jun–13 Jul	14 Jul–27 Jul		
7	Maule	19 Jun–27 Jul			
16	Ñuble	29 Mar–22 Apr			
8	Biobío	06 Apr–16 Apr			
9	Araucanía	28 Mar–08 Apr	09 Apr–29 Apr	30 Apr–14 May	22 May–05 Jun
10	Los Lagos	30 Mar–30 Apr			
11	Aysén	13 Mar–26 Mar			
12	Magallanes	26 Mar–31 Mar	01 Apr–07 May		

4 Estimation procedure

4.1 Time dependence of certain parameters

For our study, and inspired by previous work [21, 22], we assume a time-dependent transmission rate $\beta = \beta(t)$. Specifically, we assume a relationship of the type

$$\beta(t) = \beta_0\big((1-\phi)\exp(-q_\beta t) + \phi\big) \tag{6}$$

Table 7 Times t_s for the new function ρ_s.

Number	Region	Date day 1	Date day 75	t_s day for April 29
15	Arica	19 Mar	01 Jun	42
1	Tarapacá	23 Mar	06 Jun	38
2	Antofagasta	14 Mar	27 May	47
3	Atacama	14 Mar	27 May	47
4	Coquimbo	19 Mar	01 Jun	42
5	Valparaíso	16 Mar	29 May	45
13	Metropolitana	04 Mar	17 May	57
6	O'Higgins	19 Mar	01 Jun	42
7	Maule	03 Mar	16 May	58
16	Ñuble	12 Mar	25 May	49
8	Biobío	09 Mar	22 May	52
9	Araucanía	16 Mar	29 May	45
14	Los Ríos	16 Mar	29 May	45
10	Los Lagos	07 Mar	20 May	54
11	Aysén	13 Mar	27 May	47
12	Magallanes	17 Mar	30 May	44

Table 8 Times λ for quarantine periods for regions correspond to Table 6

Number	Region	λ_1	λ_2	λ_3	λ_4
15	Arica	29	14	$*$	$*$
1	Tarapacá	73	$*$	$*$	$*$
2	Antofagasta	25	14	35	$*$
5	Valparaiso	18	17	32	$*$
13	Metropolitana	50	28	14	32
6	O'Higgins	25	14	$*$	$*$
7	Maule	39	$*$	$*$	$*$
16	Ñuble	25	$*$	$*$	$*$
8	Biobío	11	$*$	$*$	$*$
9	Araucanía	12	21	15	15
10	Los Lagos	32	$*$	$*$	$*$
11	Aysen	14	$*$	$*$	$*$
12	Magallanes	6	37	$*$	$*$

that describes an exponential decline from an initial value β_0 to $\phi\beta_0$ at the rate $0 \leq q_\beta \leq 1$, where $\phi < 1$ [18, Ch. 9]. This modeling framework allows to capture early sub-exponential growth dynamics whenever $R_0 > 1$ and $q_\beta > 0$. If we assume $R_0 > 1$ in a sufficiently large susceptible population, so that the effect of susceptible depletion is negligible in the early epidemic phase, then the quantity $1 - \phi$ models the proportionate reduction in β_0 that is needed for the effective number to asymptotically reach 1.0. Hence, ϕ can be estimated as

$$\phi = \frac{1}{\beta_0 K},$$

where

$$K = \frac{q_e}{\kappa_2} + \frac{q_a q \rho_a}{\gamma_1} + \frac{q(1-\rho_s)(1-\rho_a)}{\gamma_1} + \frac{q\rho_s(1-\rho_a)}{\alpha} + \frac{h\rho_s(1-\rho_a)}{\gamma_2 + \delta},$$

and if $q_\beta = 0$, the transmission rate is constant, i.e., $\beta(t) \equiv \beta_0$.

Another special form is assumed here is for the parameter ρ_{s} that represents the proportion of fully infectious population that undergo testing, namely

$$\rho_{\mathrm{s}}(t) = \begin{cases} \rho_{\mathrm{s},1} & \text{for } t < t_{\mathrm{s}}, \\ \rho_{\mathrm{s},2} & \text{for } t \geq t_{\mathrm{s}}, \end{cases} \tag{7}$$

where $\rho_{\mathrm{s},1}$ is interpreted as the proportion of population tested before time t_{s}, and $\rho_{\mathrm{s},2}$ as the proportion of population tested afterwards. So if ρ_{s} is expressed by (7), we will have to estimate the parameters $\rho_{\mathrm{s},1}$ and $\rho_{\mathrm{s},2}$, where we would hope that occur that $\rho_{\mathrm{s},1} < \rho_{\mathrm{s},2}$, due to the increase in the number of test, being t_{s} the time in the time series that corresponds to the date 29 April for each region, with end date July 27, 2020. See Table 7 for the times t_{s} for each region.

Finally, using the information summarized in Table 6 on the quarantine periods for each regions, we may for each quarantine period defined the parameters λ asociate with each region as is detailed in Table 8, so with these values we will estimate for each λ a value for the parameter p, that represents the proportion of the susceptible population in quarantine. This process is presented in the next section, and their results in Tables 9 and 10.

4.2 Parameter estimation procedures

We now estimate some parameters of our COVID-19 model that were summarized in the previous sections and where the initial conditions satisfy

$$R(0) = Q(0) = D(0) = 0$$

along with

$$\begin{aligned} &E_1(0) = 2J(0), \quad E_2(0) = 4J(0) - E_1(0), \quad I_{\mathrm{n}}(0) = \min\{J(0), 1\}, \\ &S(0) = N - E_1(0) - E_2(0) - I_{\mathrm{n}}(0) - I_{\mathrm{s}}(0) - A(0) - J(0), \end{aligned}$$

where $J(0)$ and $I_{\mathrm{s}}(0)$ will be estimated.

Between the methods used for parameter estimation and quantifying their uncertainty, we follow two alternative approaches:

(1) One applies the Simulated Annealing (SA) method to minimize the L^2 norm between the curve C from our model and the Chilean data, with which we obtain a set to best-fit parameters. Then, using this best-fit parameter set, we realize an optimization running the least-squares method (LSQ), thus guaranteeing the global optimum. Then, using the estimated parameter set obtained by the previous step, we compute the uncertainty and the 95% confidence intervals running a bootstrap process for 250 simulations.

(2) Apply a stochastic optimization model using a classical Markov Chain Monte Carlo (MCMC) technique with the Metropolis-Hasting algorithm, where the idea is to maximize the likelihood by the stochastic search for the best parameters in a given region with a given probability distribution. During this process, we also can obtain the uncertainty of the parameters.

These two paths were chosen because both methods are powerful tools to optimize, in particular to fit models to describe epidemic phenomena with real data, such as those developed in the following works [26, 67–69]. Besides, the SA and MCMC techniques were inspired by Metropolis et al. [27], for selection for the new solutions characterized. Still, their adaptations allow applying different paradigms, one frequentist and the other Bayesian.

About the parameters to estimate we have the transmission rate β using the expression (6), where we need estimate β_0 and q_β, the diagnostic rate α, the parameters for the proportion of fully infectious individuals who undergo testing $\rho_{s,1}$ and $\rho_{s,2}$, using the expression (7) and the parameter p for identify the proportion of the population in the quarantine period λ, defined for each region with the measure declared, in otherwise the model is applied without quarantine parameters, i.e., $p = \lambda = 0$.

We incorporate the equation $C'(t)$ to the system (2) to be able to fit our model to real Chilean data, being C the sum between the symptomatic and asymptomatic or the sum between the symptomatic, asymptomatic, and without notification cumulative number cases i.e, we are considering these two situations for cumulative reported cases as our data, therefore we have two studies situations, besides, we are also considering the case of decoupled regions, i.e., we consider timelines for each region, where the first day corresponds to the first case reported and the last date assumed is July 27, 2020.

Additionally, to further guarantee the global minimum obtained to running the routine SA-LSQ (described previously in step (1)), we decide to repeat this process 20 times, assuming 20 random values drawn appropriately between the ranges defined for each parameter to estimate, as follow,

$$\begin{aligned} &0 < \beta_0 < 5, \quad 0 < q_\beta < 1, \quad 0.1 < \alpha < 2, \quad 0 < J(0) < C(0), \\ &0 < I_s(0) < 300, \quad 0 < \rho_{s,1}, \rho_{s,2} < 1, \quad \text{and } 0 < p < 1 \end{aligned}$$

(the same ranges are satisfied to apply MCMC method) being $C(0)$ is equal to first data for cases reported in each region. For this purpose, we generate these 20 values correspond to each initial parameter set, using the Matlab routine lhsdesign. Then, using these set of initial parameters we run SA fit for each one, then with these 20 estimated parameters, we select as the best-fit the one with the presnorm smaller (it is the squared 2-norm of the residual at Θ, i.e., $\sum(C(t_i, \Theta) - data_{t_i})^2$), and finally using the best-fit obtained previously, we do one run additional applying lsqcurvefit (Matlab routine) routine. With this result we can apply the bootstrap process with (250) samples . In particular, to estimate the parameters p, we assume 16 times the fits $(20 + 1)$, where the uncertainty for this parameter is increased. On the other hand, the MCMC technique was implemented to $(50 + 1k)$ samples run used Metropolis-Hastings algorithm.

Concerning the value R_0, we will use the equation (3) and the values obtained for each parameter in the estimation procedure in which each Chilean region contribute data to define a local function fitting each cumulative data, i.e., we can compute the values of R_0 for each region and later we can also compute the values for the sensitivity indexes of R_0, such as will be exposed in the section 6. Before continuing with the results, we will present the methodology necessary for the identifiability study applied to each parameter estimated and the value R_0.

5 Identifiability study

Our COVID-19 model is represented by the ODE system (2). This model has 10 epidemiological states or compartments, where we incorporate the auxiliary variable $C(t)$ that indicates the symptomatic cumulative number of diagnosed or reported new cases of the outbreak, and $C'(t)$ is the incidence of diagnosis cases. In addition to the 10 system states our model consists of 15 parameters where there are 5 classes contributing to new infectious $(E_2, A, I_\mathrm{n}, I_\mathrm{s}, J)$, and these represent the reproductive number R_0, as the sum of the contributions from each of these classes, see (3) and (5).

To begin the study of identifiability, we must follow the following steps that rely on definitions and computations presented in detail in [70] and [71]:

1. Identify and classify the parameter sets from our model. For our case, the set

$$\Theta = \{\alpha, \beta, \rho_{\mathrm{s},1}, \rho_{\mathrm{s},2}, q_\beta, p\},$$

   correspond to the parameters to be estimated, and the set

$$\Xi = \{h, q_\mathrm{e}, q_\mathrm{a}, q, \kappa_1, \kappa_2, \rho_\mathrm{a}, \gamma_1, \gamma_2, \delta, \lambda\}$$

   of parameters whose values are fixed.
2. Apply parameter estimation to obtain $\hat{\Theta}$. This is achieved by fitting our model to the C-data using either of the two approaches (the SA or the MCMC one) described in Section 4.2.
3. For each set of estimated parameters, R_0 is calculated to obtain a distribution of R_0 values as well.
4. Parameter identifiability: we say that a model parameter is identifiable from available data if its confidence interval lies in a finite range of values. Then, using the 95% confidence intervals from the distributions of each estimated parameter, we have that, if we observe a small confidence interval, this indicates that the parameter can be precisely identified, while a wider range could be indicative of lack of identifiability. In particular for the case when the confidence intervals are obtained via application of the bootstrap process, we could assess the level of bias of the estimates calculating the mean squared error (MSE) for each parameter. This quantity is calculated as

$$\mathrm{MSE} = \sum_{j=1}^{S} (\Theta - \hat{\Theta}_j)^2,$$

   where Θ represents the true parameter value (that for this case corresponds to the best-fit parameter value), and $\hat{\Theta}_j$ represents the estimated value of the parameter for the jth bootstrap realization. When a parameter can be estimated with low MSE and narrow confidence, this suggests that the parameter is identifiable from the model. On the other hand, larger confidence intervals or larger MSE values may be suggestive of non-identifiability.

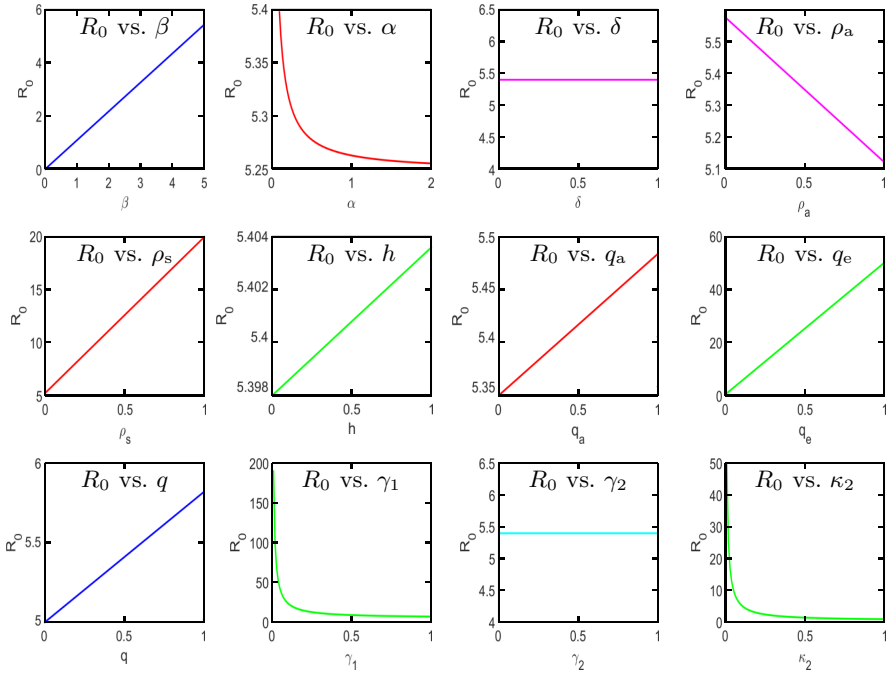

Fig. 7 Relationship between the basic reproduction number R_0 and the model parameters, where each parameter within R_0 is varied while the others are kept constant while satisfaying the conditions of Table 5

6 Sensitivity indices for R_0

This analysis is realized using the sensitivity indices defined in [72], in particular this study will be applied to R_0 to measure the relative change in a state variable when a parameter changes. This requires that we deduce closed-form expressions for the sensitivity indices of R_0 with respect to the parameters involved, where we recall that the so-called normalized forward sensitivity index Γ_p^u of a variable u that depends differentiably on a parameter p is defined as

$$\Gamma_p^u := \frac{\partial u}{\partial p} \cdot \frac{p}{u}.$$

Then, the sensitivity indices for our model are computed using our expression for R_0 presented in (3) and (5), where we utilize the parameters of Table 1. This yields the following expressions:

$$\Gamma_\beta^{R_0} = \frac{\partial R_0}{\partial \beta} \cdot \frac{\beta}{R_0} = 1 > 0, \tag{8}$$

$$\Gamma_h^{R_0} = \frac{\partial R_0}{\partial h} \cdot \frac{h}{R_0} = \frac{R^J}{R_0} > 0, \tag{9}$$

$$\Gamma_{q_e}^{R_0} = \frac{\partial R_0}{\partial q_e} \cdot \frac{q_e}{R_0} = \frac{R^{E_2}}{R_0} > 0, \tag{10}$$

$$\Gamma_{q_{\mathrm{a}}}^{R_0} = \frac{\partial R_0}{\partial q_{\mathrm{a}}} \cdot \frac{q_{\mathrm{a}}}{R_0} = \frac{R^A}{R_0} > 0, \tag{11}$$

$$\Gamma_{q}^{R_0} = \frac{\partial R_0}{\partial q} \cdot \frac{q}{R_0} = \frac{R^A + R^{I_{\mathrm{n}}} + R^{I_{\mathrm{s}}}}{R_0} > 0, \tag{12}$$

$$\Gamma_{\kappa_2}^{R_0} = \frac{\partial R_0}{\partial \kappa_2} \cdot \frac{\kappa_2}{R_0} = -\frac{R^{E_2}}{R_0} < 0, \tag{13}$$

$$\Gamma_{\rho_{\mathrm{a}}}^{R_0} = \frac{\partial R_0}{\partial \rho_{\mathrm{a}}} \cdot \frac{\rho_{\mathrm{a}}}{R_0} = \frac{R^A}{R_0} - \frac{\rho_{\mathrm{a}}(R^{I_{\mathrm{n}}} + R^{I_{\mathrm{s}}} + R^J)}{(1-\rho_{\mathrm{a}})R_0} < 0, \tag{14}$$

$$\Gamma_{\rho_{\mathrm{s}}}^{R_0} = \frac{\partial R_0}{\partial \rho_{\mathrm{s}}} \cdot \frac{\rho_{\mathrm{s}}}{R_0} = \frac{R^{I_{\mathrm{s}}} + R^J}{R_0} - \frac{\rho_{\mathrm{s}} R^{I_{\mathrm{n}}}}{(1-\rho_{\mathrm{s}})R_0} > 0, \tag{15}$$

$$\Gamma_{\alpha}^{R_0} = \frac{\partial R_0}{\partial \alpha} \cdot \frac{\alpha}{R_0} = -\frac{R^{I_{\mathrm{s}}}}{R_0} < 0, \tag{16}$$

$$\Gamma_{\gamma_1}^{R_0} = \frac{\partial R_0}{\partial \gamma_1} \cdot \frac{\gamma_1}{R_0} = -\frac{(R^A + R^{I_{\mathrm{n}}})}{R_0} < 0, \tag{17}$$

$$\Gamma_{\gamma_2}^{R_0} = \frac{\partial R_0}{\partial \gamma_2} \cdot \frac{\gamma_2}{R_0} = -\frac{R^J \gamma_2}{R_0(\gamma_2 + \delta)} < 0, \tag{18}$$

$$\Gamma_{\delta}^{R_0} = \frac{\partial R_0}{\partial \delta} \cdot \frac{\delta}{R_0} = -\frac{R^J \delta}{R_0(\gamma_2 + \delta)} < 0. \tag{19}$$

These sensitivity indices of R_0 can be positive or negative. Since all indices are functions of other parameters, the sensitivity indices will change with other parameter values. We will show a particular analysis with the values of parameters estimated applied to regional Chilean data in Section 7.

But before, using the model parameters and R_0 expression, which we know are positive values and R_0 greater than R^A, R^{E_2}, $R^{I_{\mathrm{s}}}$, $R^{I_{\mathrm{n}}}$, R^J; where obtain the positive and negative signs shown together to the sensitivity indices in expressions (8)–(19) the which represent the following, if the index is positive, we have a relationship directly proportional between R_0 and the parameter analyzed, i.e., if the parameter increases the R_0 increases. On the contrary, if the sign is negative, the relationship will be the opposite, i.e., if the parameter increases, then R_0 decreases. Besides, Figure 7 illustrates the sensitivity of the parameters that define the parameter R_0, where we can observe the following.

The parameters β, h, q_{e}, q_{a}, q, and ρ_{s} are more sensitive to control the transmission of the disease since a small increase in these parameters imply an increase of R_0 significantly, especially for the parameters q_{e}, ρ_{s}, where for a small increase of them, the value for R_0 is varying by more than 10 units. A similar situation occurs with the parameter ρ_{a}, but in an opposite sense, where a small increase in this parameter implies a significant decrease of R_0. For the case of parameters γ_1, κ_2, and α, we can see that the relationship is inversely proportional with R_0, where if these values increase, therefore the disease fatality starts to decrease with time. This could be translated as a reduction in the times $1/\gamma_1$, $1/\kappa_2$, and $1/\alpha$ imply a reduction in the R_0 value. Finally, we have that R_0 is not very sensitive to the parameters δ and γ_2, due to dependence of these indices with R^J especially with the parameter h which was fixed equal to zero.

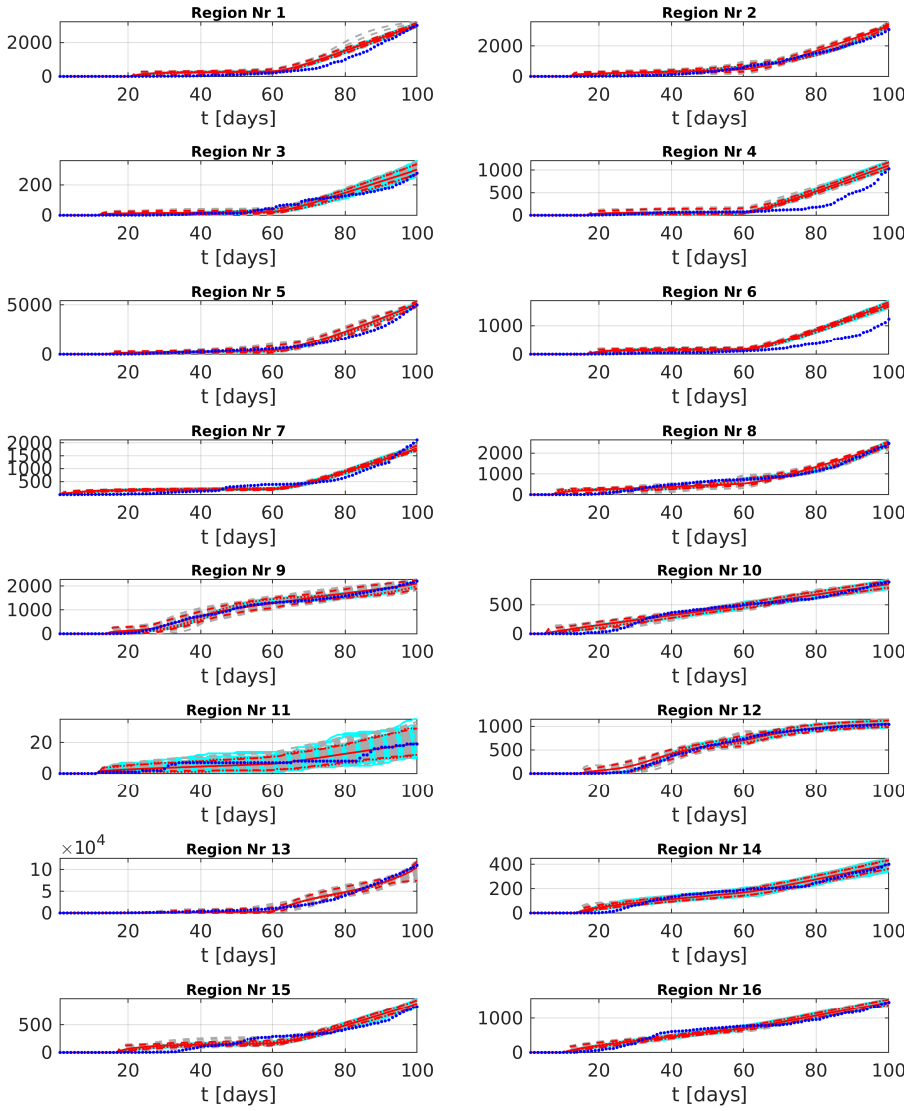

Fig. 8 Fit of the model (2) to compartment C based on the reported symptomatic and asymptomatic cases, and using the SA method. Here and in Figure 9, cumulative cases are depicted in blue dots, fit curves are the red lines, the 95% CIs are the dashed red lines and cyan curves correspond to simulated curves generated during the bootstrap process

7 Results

Our study considers the daily cumulative COVID-19 cases reported in Chile for its 16 regions. For the model fit, we assume two versions of the data at the moment of calibration. The first version considers as data the sum of the daily cumulative cases reported for symptomatic and asymptomatic cases because various asymptomatic cases reported can be symptomatic later. In the second version the data are

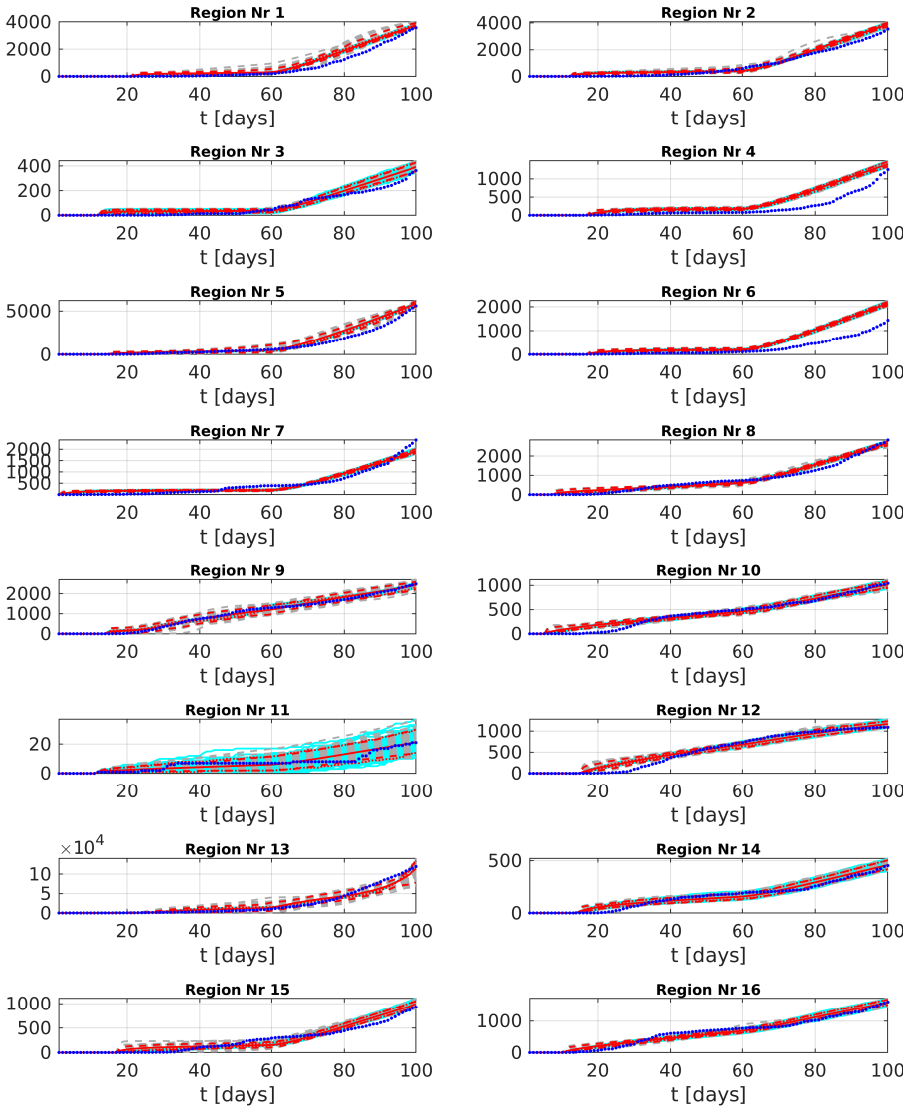

Fig. 9 Fit of the model (2) to compartment C based on the reported symptomatic, asymptomatic, and without-notifying cases, and using the SA method.

taken as the sum of the daily cumulative cases reported for symptomatic, asymptomatic, and without-notification cases. We recall that the "without-notification" cases are those with a positive PCR test with or without symptoms. With respect to timeline; we assume one for each region, the first date is that of the first case and the last cases are assumed for July 27, of 2020. We estimate unknown model parameters such as the transmission rate β, the time α from symptom onset to isolation or hospitalization, the proportion ρ_s of fully infectious individuals who undergo testing and the proportion p of the susceptible population in quarantine declared. To estimate the parameters β and ρ_s we employ the expressions (6)

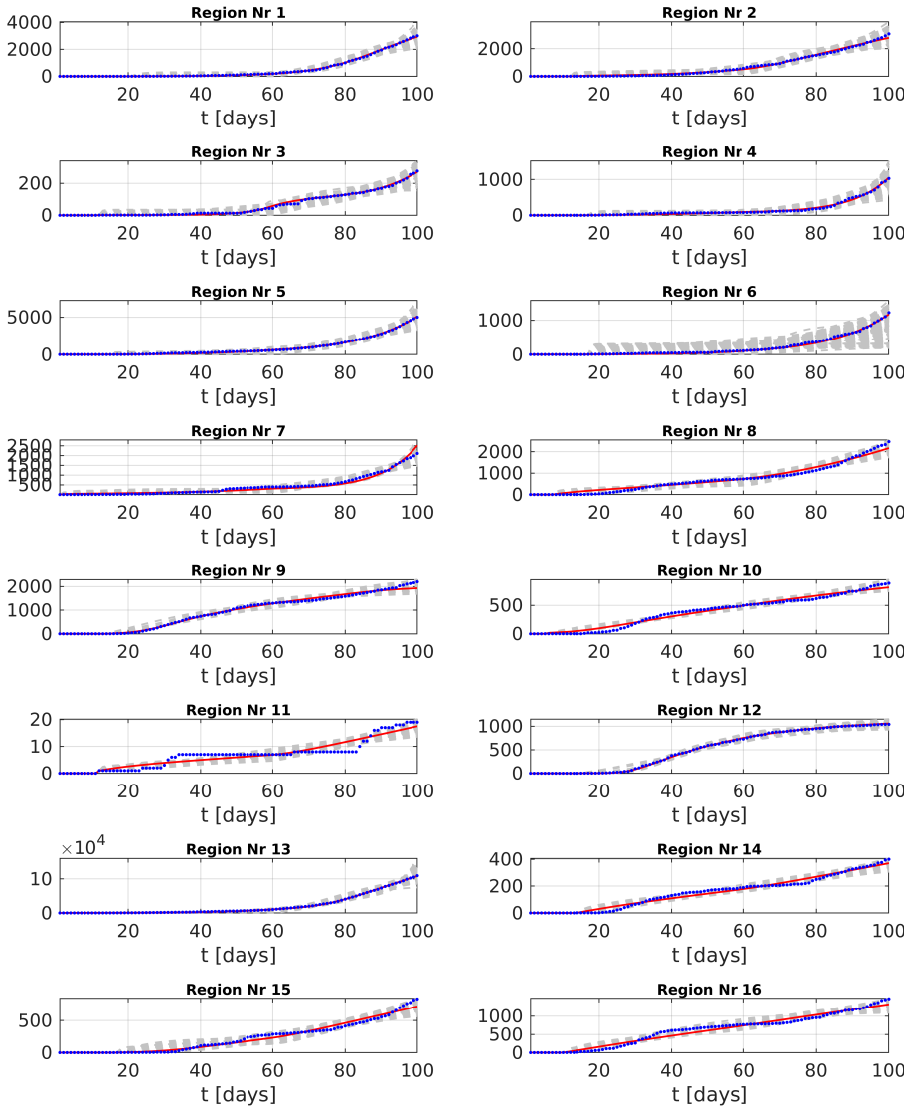

Fig. 10 Fit of the model (2) to compartment C based on the reported symptomatic and asymptomatic cases, and using the MCMC method. Here and in Figure 11, cumulative cases are depicted in blue dots, fit curves are the red lines, and the 95% CIs are the dashed gray lines

and (7), respectively, where it becomes necessary to estimate the parameters β_0 and q_β (for β) as well as $\rho_{s,1}$ and $\rho_{s,2}$ (for ρ_s). Moreover, the quarantine parameter p depends on each region because this control measure was applied in different moments and periods in each region (see Table 6). Some unknown initial conditions of our model (2) are also are estimated for each version of data. Then, following the process exposed in Section 4, we now present the results obtained for the estimation of the parameters and their uncertainty along with the sensitivity

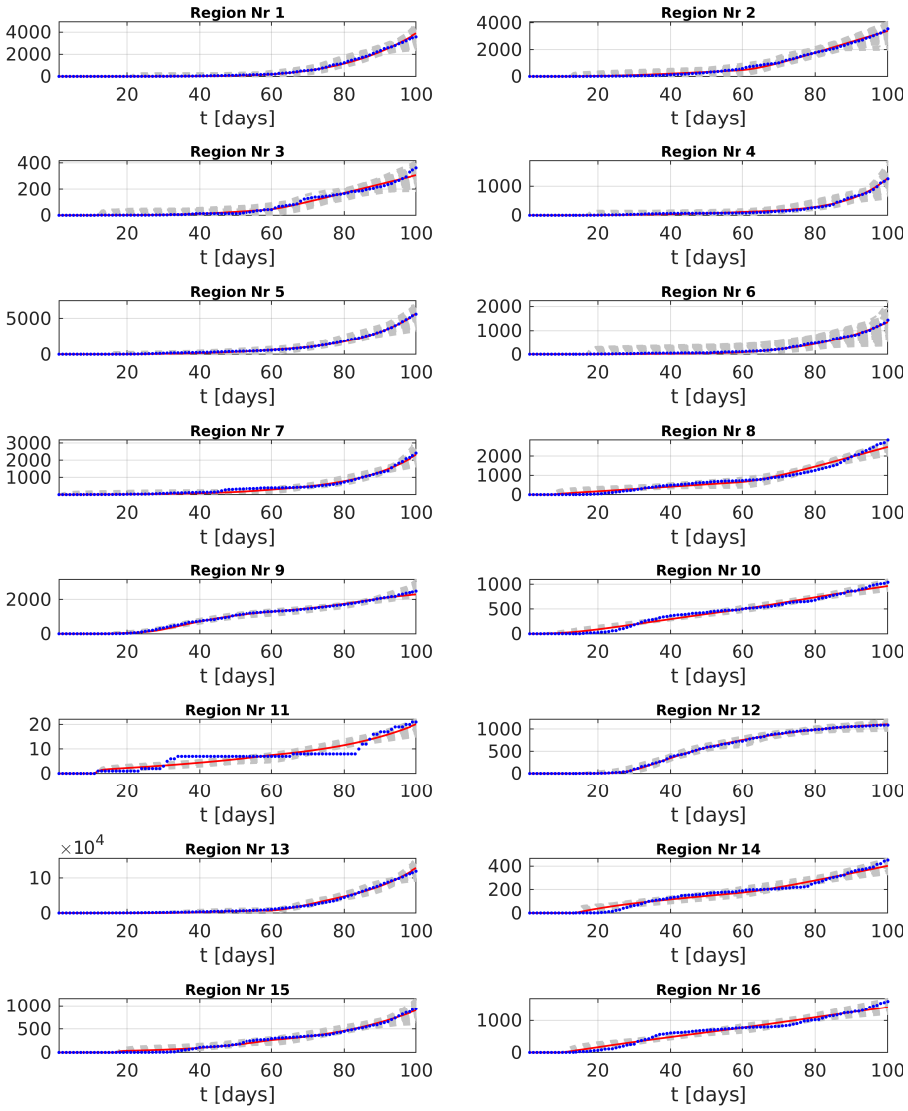

Fig. 11 Fit of the model (2) to compartment C based on the reported symptomatic, asymptomatic, and without-notifying cases, and using the MCMC method.

analysis for the basic reproductive number R_0, using the results obtained for the parameters estimated for each region.

7.1 Parameter estimation

Using the SA method and the least-squares optimization, we obtained the estimated parameters summarized in Table 9, and we used the bootstrapping process for the computation of their 95% confidence intervals summarized in Tables 11

and 13, and plotted in Figures 8 and 9. The analogous results arising from using the stochastic optimization MCMC method applying the Metropolis-Hastings algorithm are presented in Table 10 with their respectively 95% confidence intervals shown in Tables 12 and 14 and plotted in Figures 10 and 11. In light of the results shown in these figures and tables it appears that the fits obtained are acceptable for both versions of the data and for the two optimization processes applied, because in the majority of cases the parameters estimated are relatively close, evidencing possibly an identification of our best-fit parameters. This observation is discussed in more detail in the next section.

7.2 Identifiability analysis

Studying the results for the mean and the 95% confidence intervals, summarized in Tables 11 to 13 for the bootstrapping process and in Tables 12 to 14 with the MCMC process, we can observe the following. For both methodologies, those based on SA and those based on MCMC, the 95% confidence intervals have finite ranges and in almost all cases the mean value maintains a central position in theses intervals which suggests that the parameters are being identifiable. In particular for $I_s(0)$ and R_0 intervals, have a wide range, opposite to intervals obtained to q_β for example, which intervals have a close range. Observing the $\rho_{s,1}$ and $\rho_{s,2}$ intervals, we can note that the parameter $\rho_{s,1}$ has a trend to left side of intervals, and the $\rho_{s,2}$ to the right side, suggesting that effectively the relation $\rho_{s,1} < \rho_{s,2}$ is satisfied for the majority cases. Besides studying the MSE values for the $I_s(0)$ and R_0 intervals generated with the bootstrap process, we observe that the values for R_0 are between the range $[12, 70]$ and for $I_s(0)$ between $[2, 30000]$, possibly these rather large ranges are due to that in particular these parameters strongly depend on the population behavior, control measures, and collected process of data. The identifiability of parameters is in occasions an problem because, as is mentioned in [70], when structural identifiability is not an issue, a parameter may still be non-identifiability in practice due to other factors, such as the amount and quality of the data available and the number of parameters that are jointly estimated from the available data. This last part can be difficult in our case because of the multiple changes in the criteria for collecting data around the COVID-19 crisis. Reason by the to future experiments, we hope to explore more data and parameters

7.3 Sensitivity analysis

The indices in the expressions (8)-(19) computed between the basic reproduction number R_0 and the parameters involved can help us assessing the impact of each parameter to the value of R_0, which indicates whethe the COVID-19 will continue to propagate in each Chilean region or not. Then, using the parameters estimated for each region, method, and data, as well as the fixed and assumed parameters in Table 5, we can see the following results, summarized in Tables 15 and 16 and Figures 12 and 13.

The fact that for all regions and situations $\Gamma_\beta^{R_0} = 1$ means that if we increase (or decrease) 10% in β, keeping other parameters fixed, will produce 10% increase (or decrease) in R_0. Similarly, for each positive index, for example, the index $\Gamma_{\rho_s}^{R_0}$

for region 13, and model SA, we obtained the values 0.0046 and 0.0360 respectively, whereby if increasing (or decreasing) a 10% the parameter involved, increases (or decrease) R_0 by $0,046\%$ and 0.360% respectively, having an impact greater the parameter ρ_{s} when the parameters are estimated using the data with symptomatic, asymptomatic and without notification than using the data with symptomatic and asymptomatic. Now, if the index is negative, like appear for example for index $\Gamma_{\rho_{\mathrm{a}}}^{R_0}$ for region 13, and model MCMC, we obtained the values -0.2507 and -0.0746 respectively, an increasing (or decreasing) by 10% for parameter ρ_{a} implies decreases (or increases) for R_0 by 2.507% and 0.746% respectively, being the effect greater for parameter ρ_{a} when the other parameters are estimated using the data with symptomatic and asymptomatic than using the data with symptomatic, asymptomatic and without notification.

A different situation occurs when the sensitivity index is equal to zero like in $\Gamma_h^{R_0}$, $\Gamma_{\gamma_2}^{R_0}$ and $\Gamma_\delta^{R_0}$ which means that these parameters do not affect R_0. This situation occurs for the assumption $h = 0$.

Analyzing Figures 12 and 13, we can see that regions 2 and 5 have a smaller sensitivity than regions 12 and 16, which indicates that the value for R_0 is affected more intensely for these regions. Another observation in this part is that the values for sensitivity indices present different behavior for each region. We can say that the regions with bars with close heights for each parameter, the selection of the model, and the data represent the same impact of sensitivity. But in the cases when the bars have variable heights, as in region 1, we can say in this case that the MCMC model contributes more sensitivity for the parameters q, ρ_{a}, ρ_{s}, and α than the SA model.

8 Conclusions

In this paper, we analyze and adapt a model propose for the outbreak of COVID-19 for the Chilean case, where we incorporate the dynamic quarantines declared for the national government for each one Chilean region, which follow a control strategy particularly defined for each region, for example, the region 13 named Metropolitana, applied measures of quarantine of reinforcing, and on the other hand region 9 named Araucana, applied quarantines of relaxation, i.e., the measure was applied incorporating more or less regional population in each case. Using this model, information of population with positive COVID-19 test, and the dates of quarantine applied for each region, we estimate unknown parameters using two paths, one with an SA algorithm as a minimization procedure and the other with an MCMC algorithm as a stochastic optimization procedure. Our studies have shown optimal results for the fits of data to our model, wherewith the parameters estimated, we also study the contribution of each parameter involving in the definition of the basic reproduction number R_0, including the compute of sensitivity indices, which indicate us that the sensitivity level depends on each region, due to that is observing more sensibility in some regions than others, which can indicate us that the quality of data is different for each region, where possibly also is depending on factors such as accessibility, connectivity, and the density population which could possibly hinder the fit methodologies, then to improve these factors we could include more data sources, reducing the number of parameters estimated, or implement some extension of our optimization methods. Then, a next goal to

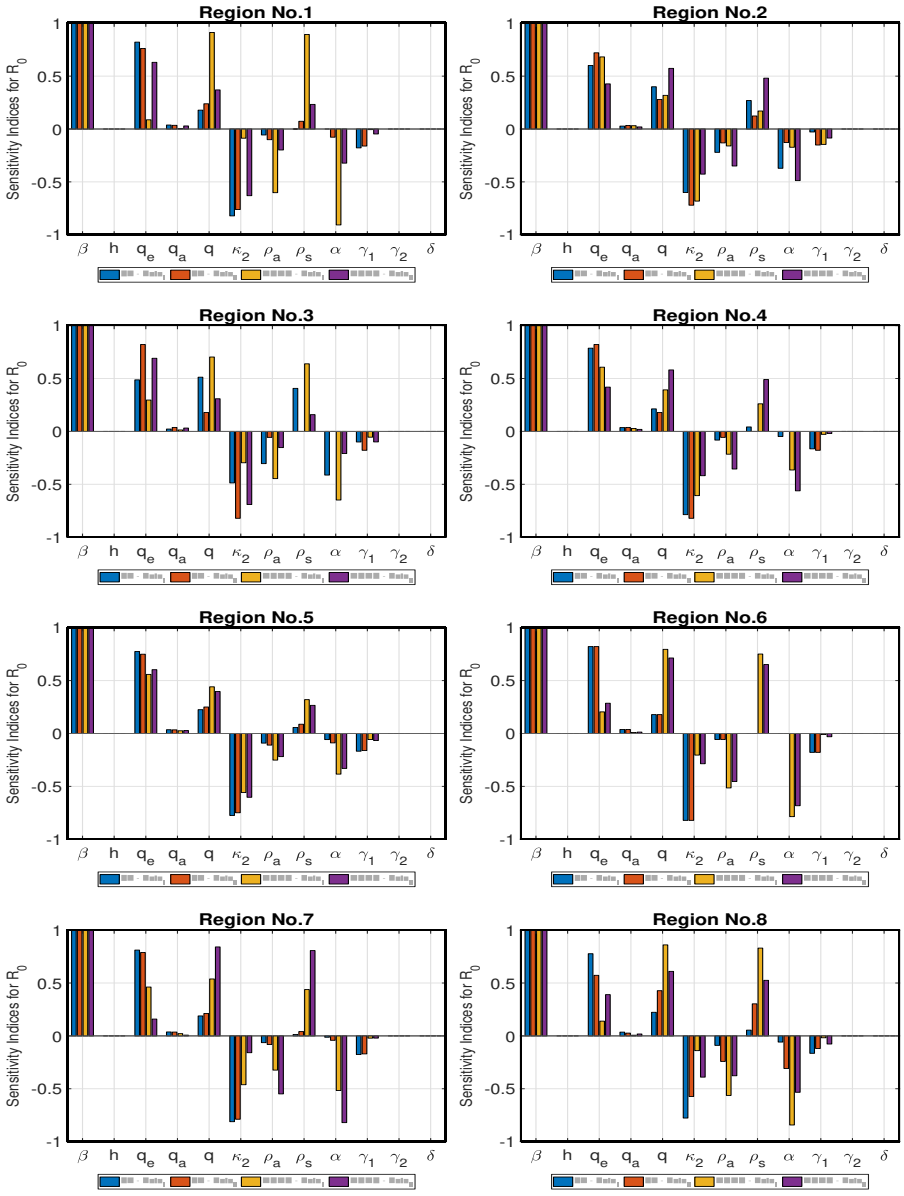

Fig. 12 Values for the sensitivity indices between the basic reproduction number R_0 with their parameters, applied for each Chilean region

improve our study could be to include the possibilities mentioned before and generate forecasts, a tool of utility for the create control policies; as well as applying our model to countries that involve dynamic quarantines like Chile have applied.

Acknowledgements RB is supported by Fondecyt project 1170473; CMM, project ANID/PIA/AFB170001; and CRHIAM, project ANID/FONDAP/15130015. GC is partially supported

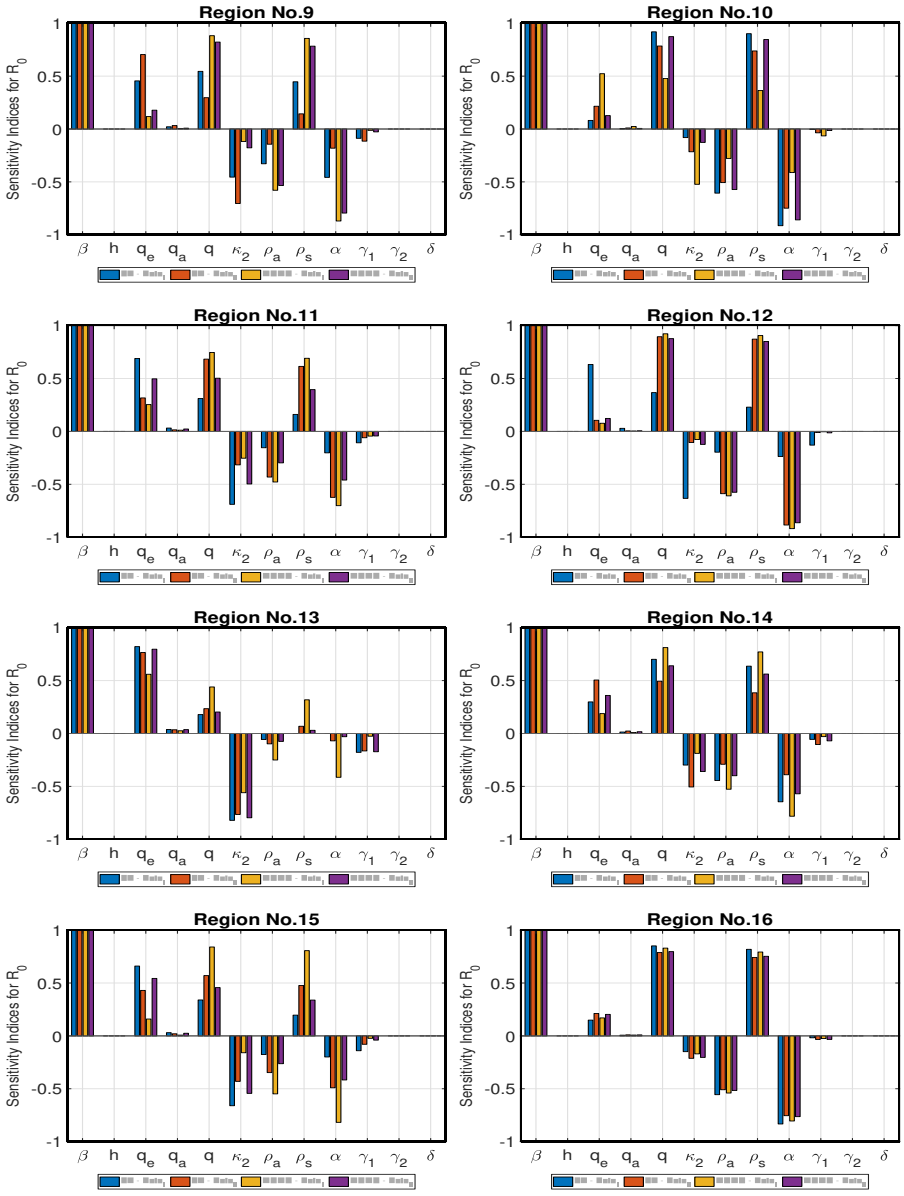

Fig. 13 Values for the sensitivity indices between the basic reproduction number R_0 with their parameters, applied for each Chilean region.

by NSF grants #2026797, #2034003, and NIH R01 GM 130900. IK would like to thank the German Research Foundation (DFG) for financial support of the project within the Cluster of Excellence Data-Integrated Simulation Science (EXC 2075), DFG Project 432343452. LYLD is supported by ANID scholarship ANID-PCHA/Doctorado Nacional/2019-21190640.

Appendix: Tables

Table 9 Parameter estimation results, using SA method, where for each region the estimation is computed for compartment C using cases reported of symptomatic and asymptomatic (first row per region), and symptomatic, asymptomatic, and without-notifying (second row per region), where the times fitted correspond to 100 days for each region

Region	α	β_0	$\rho_{s,1}$	$\rho_{s,2}$	q_β	$I_s(0)$	$J(0)$	R_0	p_1	p_2	p_3	p_4
1	0.1581	4.8443	1.70E-06	0.8097	0.4622	264.3532	0.6112	14.0970	3.16E-10	0.0000	0.0000	0.0000
	0.3956	1.8415	0.0335	0.5523	0.0921	151.1597	0.7011	5.2759	8.87E-10	0.0000	0.0000	0.0000
2	1.9293	1.4619	0.9943	0.9837	0.0000	122.0719	0.4325	1.4276	2.84E-05	0.9656	0.9560	0.0000
	0.2785	0.8017	0.0413	0.6894	0.0427	292.8014	0.0780	2.2991	2.87E-06	0.2038	0.3167	0.0000
3	0.1000	2.6314	0.0706	0.6463	0.1040	2.9064	0.3551	7.8246	0.0000	0.0000	0.0000	0.0000
	1.0704	4.3201	1.05E-10	1.0000	0.5751	30.9249	0.8290	12.5714	0.0000	0.0000	0.0000	0.0000
4	0.8716	1.3734	0.0443	0.6350	0.0522	17.6875	1.9906	3.8899	0.0000	0.0000	0.0000	0.0000
	0.1452	4.6505	1.55E-08	0.9941	0.7929	169.1270	1.9186	13.5330	0.0000	0.0000	0.0000	0.0000
5	0.1001	3.9084	0.0062	0.9517	8.24E-05	236.9431	0.9570	11.3949	0.6196	0.3269	2.24E-05	0.0000
	0.1002	4.8354	0.0099	0.6895	3.73E-06	284.2471	0.0141	14.1139	0.7437	0.2986	3.32E-01	0.0000
6	0.1888	1.3813	1.78E-12	0.8694	0.1372	146.6748	0.0778	4.0195	0.8975	0.0000	0.0000	0.0000
	0.1000	4.6401	4.49E-10	0.8401	0.4099	189.5636	1.1623	13.5026	0.6243	0.0000	0.0000	0.0000
7	0.1003	1.8135	0.0013	0.0919	0.0761	199.0074	0.1154	5.2793	0.9645	0.0000	0.0000	0.0000
	0.1704	3.0562	0.0075	0.9998	0.3956	175.7557	0.0376	8.8859	0.1750	0.0000	0.0000	0.0000
8	0.4728	0.9673	0.0296	0.0060	0.0050	230.5518	0.0204	2.7731	0.0075	0.0000	0.0000	0.0000
	0.1184	3.3225	0.0531	0.2627	0.1729	165.3615	0.8245	9.7452	0.0001	0.0000	0.0000	0.0000
9	0.1663	2.0137	0.1393	0.1158	0.0029	102.7795	0.0382	5.7770	0.2038	0.9321	0.1435	0.1050
	1.4701	2.7496	0.3155	0.0816	0.0043	139.9054	0.3853	6.3564	0.9499	0.0618	0.3038	0.1612
10	0.1000	2.1531	0.9384	0.9919	0.7343	82.2277	0.9911	8.0834	0.0002	0.0000	0.0000	0.0000
	0.1001	3.9754	0.2902	0.9235	0.9617	144.5329	0.7966	12.6036	0.0032	0.0000	0.0000	0.0000
11	1.4522	2.2429	0.3559	0.8175	0.6290	0.5264	0.4983	5.0155	3.61E-06	0.0000	0.0000	0.0000
	0.1000	4.0574	0.1642	0.6089	4.80E-05	1.1781	0.7712	12.4067	0.8031	0.0000	0.0000	0.0000
12	0.2306	4.7867	0.0720	0.3660	0.0022	11.9593	0.2933	13.6539	0.1803	0.7337	0.0000	0.0000
	0.1000	0.3433	0.7043	0.8504	0.3802	287.1273	1.0324	1.2166	0.0062	0.0034	0.0000	0.0000
13	1.4442	4.0760	0.0005	0.3746	1.62E-05	298.2031	0.4250	11.8576	0.2369	0.0019	0.1368	0.6008
	0.1372	4.9718	0.0104	0.9874	3.40E-06	35.5397	0.0056	14.4726	0.7719	0.0395	0.6804	0.8227
14	0.1000	1.3675	0.1803	0.4954	0.2878	81.6854	0.2541	4.2014	0.0000	0.0000	0.0000	0.0000
	0.1000	2.8864	0.0643	0.3598	0.4024	97.4858	0.4738	8.5664	0.0000	0.0000	0.0000	0.0000
15	0.1097	3.0168	0.0276	0.9718	0.6072	141.0256	0.1396	8.8319	2.32E-09	0.0000	0.0000	0.0000
	0.1993	2.9098	0.1895	0.9177	0.2047	33.7114	0.2317	8.1396	4.15E-07	0.0000	0.0000	0.0000
16	0.1210	1.5486	0.5633	0.9804	0.6570	203.7960	0.3003	4.8370	2.05E-10	0.0000	0.0000	0.0000
	0.1175	4.3870	0.3483	0.9976	0.9912	199.6158	0.4585	13.4599	0.0034	0.0000	0.0000	0.0000

Table 10 Parameter estimation results. Same information as Table 9 but obtained by MCMC method

Region	α	β_0	$\rho_{s,1}$	$\rho_{s,2}$	q_β	$I_s(0)$	$J(0)$	R_0	p_1	p_2	p_3	p_4
1	0.1000	0.6786	0.8693	0.9965	0.0025	14.9960	0.0166	2.5049	0.0889	0.0000	0.0000	0.0000
	1.9537	1.7802	0.8333	0.9945	0.0031	0.3507	0.8232	2.2929	0.0067	0.0000	0.0000	0.0000
2	0.1000	2.6153	0.0211	0.0631	0.0752	97.2816	1.9938	7.6602	0.0001	0.5428	0.9983	0.0000
	0.1051	4.3629	0.1002	0.7894	0.1751	47.6641	0.2666	13.0262	0.0016	0.9182	0.8943	0.0000
3	0.1054	1.1898	0.1922	0.0026	0.0002	0.4499	0.0996	3.6329	0.0000	0.0000	0.0000	0.0000
	1.6989	4.9987	0.4282	0.9131	0.0876	0.1587	0.0165	10.4296	0.0000	0.0000	0.0000	0.0000
4	1.9970	1.3637	1.0000	0.5846	0.0008	0.0740	1.9984	1.3095	0.0000	0.0000	0.0000	0.0000
	0.8932	1.2198	0.9986	0.6462	0.0005	0.1014	1.9997	1.4009	0.0000	0.0000	0.0000	0.0000
5	1.1705	5.0000	0.6709	0.5125	2.02E-06	4.7297	0.5085	8.3657	0.2485	0.0000	2.34E-07	0.0000
	1.3634	4.9935	0.6220	0.4975	0.0008	0.1169	0.9991	8.6915	0.2386	0.9983	0.9966	0.0000
6	0.3117	0.9715	0.9993	0.8680	0.0034	0.9177	0.9194	1.7228	0.0021	0.0000	0.0000	0.0000
	0.3217	0.8620	0.6400	0.9979	0.0018	0.2743	1.5039	1.8645	0.8075	0.0000	0.0000	0.0000
7	1.0693	1.2341	0.9973	0.4683	0.0013	35.1774	0.0703	1.3518	0.1259	0.0000	0.0000	0.0000
	0.1168	0.6199	0.5022	0.2993	0.0003	11.9887	0.8376	1.9495	0.9585	0.0000	0.0000	0.0000
8	0.1036	0.3468	0.5213	0.9984	0.0007	246.6453	0.0886	1.1530	0.0005	0.0000	0.0000	0.0000
	0.1032	2.3107	0.1176	0.6061	0.1920	183.9942	0.1601	6.9432	0.0003	0.0000	0.0000	0.0000
9	0.1045	4.9927	0.6442	0.6914	0.2798	75.1113	0.1216	17.0058	0.1005	0.0006	7.14E-07	0.6371
	0.1010	1.9525	0.3759	0.7818	9.04E-05	86.4802	0.0051	6.3197	0.8660	0.6383	0.2746	0.9978
10	0.8241	4.2548	0.5410	0.5795	0.1763	22.3958	0.3148	8.3858	0.0048	0.0000	0.0000	0.0000
	0.1099	3.0349	0.6216	0.9996	0.2659	34.2630	0.9985	10.0176	0.0046	0.0000	0.0000	0.0000
11	0.1070	0.7144	0.2470	0.9663	1.0000	2.3599	0.6058	2.2032	0.0007	0.0000	0.0000	0.0000
	0.9874	0.7855	0.7616	0.5886	2.40E-06	0.6709	0.1888	1.2113	0.0016	0.0000	0.0000	0.0000
12	0.1004	5.0000	0.9990	0.9961	0.0018	0.1685	0.8483	18.9902	1.0000	0.7981	0.0000	0.0000
	0.1066	4.9956	0.6254	0.8320	0.0010	0.3602	1.4181	16.7691	0.9724	0.7116	0.0000	0.0000
13	1.6195	1.8723	0.9983	0.7686	0.0036	280.1964	0.0034	1.8695	0.0012	0.0603	1.0000	0.0012
	0.1069	4.9962	0.0034	0.1764	9.15E-08	2.3289	0.6578	14.5511	0.1303	0.0018	0.8885	0.3041
14	0.1000	4.0923	0.3470	0.5644	1.0000	56.0864	0.9994	13.1865	0.0000	0.0000	0.0000	0.0000
	0.1032	5.0000	0.1363	0.3420	0.6878	73.7061	0.0422	15.1000	0.0000	0.0000	0.0000	0.0000
15	0.1000	3.4252	0.4275	0.8700	0.1975	15.9374	0.1144	11.2852	3.86E-06	0.0000	0.0000	0.0000
	1.3127	1.3803	0.8388	0.4544	0.0159	32.2072	0.9525	1.8500	0.0050	0.0000	0.0000	0.0000
16	0.1021	4.9867	0.4026	0.4743	0.8508	167.6240	0.0269	16.1927	0.0017	0.0000	0.0000	0.0000
	0.1018	4.9767	0.3187	0.4036	0.6775	176.0414	2.02E-07	15.8265	0.0012	0.0000	0.0000	0.0000

Table 11 Confidence intervals for estimated parameters α β_0, $\rho_{s,1}$, $\rho_{s,2}$, q_β using SA method. For each region the estimates are computed using cases reported of symptomatic and asymptomatic (first row per region), and symptomatic, asymptomatic, and without-notifying (second row per region) individuals, based on regional data from Chile

Region	α mean 95%CI	β_0 mean 95%CI	$\rho_{s,1}$ mean 95%CI	$\rho_{s,2}$ mean 95%CI	q_β mean 95%CI	R_0 mean 95%CI
1	0.5065 (0.1039,1.8676)	3.2385 (0.6590,4.9964)	0.0599 (1.57E-08,0.5080)	0.8614 (0.3929,1.0000)	0.3212 (0.0021,0.6945)	9.2620 (1.8762,14.5356)
	0.6319 (0.1000,1.8172)	3.1006 (0.6627,4.9855)	0.0730 (1.69E-09,0.5427)	0.8330 (0.2165,1.0000)	0.2309 (0.0008,0.5446)	8.8438 (1.7553,14.3616)
2	0.4822 (0.1003,1.9051)	2.7047 (0.5546,4.9771)	0.1498 (0.0100,0.9492)	0.7677 (0.0484,0.9998)	0.2391 (3.03E-05,0.6714)	7.5651 (1.4699,14.2568)
	0.5629 (0.1133,1.8981)	3.3839 (0.6676,4.9879)	0.0595 (0.00474,0.2368)	0.8387 (0.2810,1.0000)	0.2868 (0.0037,0.5901)	9.6277 (1.7709,14.3329)
3	0.6735 (0.1002,1.8475)	3.5036 (0.8947,4.9993)	0.0365 (3.37E-14,0.2027)	0.8273 (0.1895,1.0000)	0.2805 (0.0317,0.7177)	10.0679 (2.4323,14.5482)
	0.7896 (0.1290,1.8714)	3.5301 (0.8644,4.9986)	0.0190 (2.33E-14,0.1179)	0.8794 (0.3210,1.0000)	0.4177 (0.0432,0.9411)	10.1777 (2.4940,14.5453)
4	0.5369 (0.1000,1.6148)	3.4403 (0.8445,4.9999)	0.0143 (2.35E-14,0.1267)	0.8709 (0.1642,1.0000)	0.3130 (0.0366,0.8614)	9.9732 (2.4073,14.5496)
	0.3207 (0.1020,1.3599)	3.7121 (1.1356,4.9977)	0.0193 (4.14E-14,0.1083)	0.9039 (0.4371,1.0000)	0.5739 (0.0536,0.9829)	10.7379 (3.2515,14.5099)
5	0.4567 (0.1000,1.8584)	3.2470 (0.6893,4.9871)	0.0777 (1.32E-06,0.6994)	0.6829 (0.0962,0.9998)	0.0850 (2.63E-12,0.4112)	9.2881 (1.8610,14.5535)
	0.4801 (0.1000,1.8952)	3.0972 (0.7827,4.9933)	0.0819 (2.24E-05,0.5163)	0.6730 (0.0941,0.9987)	0.0771 (1.28E-11,0.3731)	8.8873 (1.9859,14.5559)
6	0.4148 (0.1052,1.6094)	3.4489 (0.7455,4.9934)	0.0149 (2.43E-14,0.1225)	0.8971 (0.3618,1.0000)	0.4208 (0.0357,0.8839)	9.9874 (2.0569,14.5307)
	0.3417 (0.1002,1.2586)	3.4998 (0.8158,4.9984)	0.0184 (3.25E-14,0.1235)	0.9015 (0.3504,1.0000)	0.3958 (0.0339,0.8777)	10.1359 (2.3756,14.5449)
7	0.2284 (0.1000,0.8223)	3.7059 (1.0328,4.9943)	0.0184 (6.70E-13,0.0799)	0.8774 (0.2728,1.0000)	0.4667 (0.0680,0.8615)	10.7275 (3.0039,14.5364)
	0.3227 (0.1063,0.9582)	3.5397 (0.5815,4.9978)	0.0144 (2.11E-11,0.0640)	0.9047 (0.4187,1.0000)	0.4317 (0.0227,0.8327)	10.2466 (1.6607,14.5302)
8	0.4379 (0.1010,1.7144)	3.2638 (0.5922,4.9773)	0.1724 (0.0345,0.7316)	0.7942 (0.0560,0.9999)	0.4137 (0.0002,0.9320)	9.0226 (1.4578,14.3560)
	0.4822 (0.1001,1.6742)	3.4069 (0.7584,4.9887)	0.1631 (0.0375,0.4113)	0.7845 (0.2297,0.9984)	0.3141 (0.0265,0.8112)	9.3614 (2.0113,14.2923)
9	0.8177 (0.1000,1.9613)	3.3583 (1.0251,4.9701)	0.2798 (0.0061,0.9868)	0.3767 (0.0049,0.9832)	0.0739 (1.49E-11,0.9674)	9.0658 (2.9850,17.1168)
	0.8982 (0.1000,1.9543)	3.4133 (1.1767,4.9933)	0.2429 (0.0060,0.9665)	0.4268 (0.0052,0.9905)	0.0822 (2.80E-09,0.9195)	9.2282 (2.4368,15.3049)
10	0.2633 (0.1000,1.7517)	2.0549 (0.0300,4.9742)	0.6036 (0.0481,0.9970)	0.7687 (0.2604,0.9993)	0.5510 (0.0048,0.9915)	6.0344 (0.1018,15.6254)
	0.3574 (0.1000,1.8852)	2.6458 (0.4205,4.8919)	0.3409 (0.0535,0.7124)	0.7928 (0.2072,1.0000)	0.5490 (0.0734,0.9894)	7.0912 (1.3234,14.0082)
11	0.8878 (0.1001,1.9666)	2.4830 (0.0592,4.9433)	0.2325 (0.0064,0.6906)	0.7377 (0.2182,0.9999)	0.5466 (0.0004,0.9959)	6.4950 (0.1424,14.1760)
	0.5301 (0.1000,1.8226)	2.6534 (0.1420,4.9829)	0.1837 (7.78E-05,0.5620)	0.7318 (0.1634,0.9963)	0.5183 (5.69E-07,0.9913)	7.3141 (0.3883,14.9754)
12	0.5913 (0.1000,1.9604)	3.8978 (0.6623,4.9947)	0.2726 (0.0059,0.9962)	0.5485 (0.0197,0.9970)	0.1164 (8.77E-08,0.9492)	10.9909 (2.1327,17.1301)
	0.3070 (0.1000,1.8479)	2.1434 (0.0228,4.9792)	0.5772 (0.0159,0.9905)	0.7008 (0.1751,0.9938)	0.5326 (0.0002,0.9916)	5.7962 (0.0848,14.6020)
13	1.1482 (0.1024,1.9911)	3.8294 (1.1802,4.9945)	0.0361 (8.85E-08,0.5631)	0.6129 (0.0657,0.9920)	0.0030 (4.42E-11,0.0385)	11.0264 (2.5729,14.5228)
	1.0962 (0.1019,1.9801)	3.7847 (1.0419,4.9915)	0.1053 (0.0021,0.9740)	0.5376 (0.0652,0.9922)	0.0024 (6.92E-14,0.0164)	10.6693 (2.2540,14.4774)
14	0.3787 (0.1000,1.4088)	2.3968 (0.1259,4.7381)	0.3860 (0.0920,0.7073)	0.7843 (0.2330,1.0000)	0.5388 (0.1136,0.9707)	5.8657 (0.3911,11.8709)
	0.2899 (0.1000,1.2692)	2.1787 (0.2739,4.6800)	0.2113 (0.0327,0.4901)	0.8168 (0.3517,1.0000)	0.5859 (0.0676,0.9870)	5.8355 (0.8063,12.4525)
15	0.4266 (0.1000,1.8993)	3.4411 (0.8394,4.9964)	0.0555 (1.28E-07,0.2278)	0.8833 (0.4684,1.0000)	0.6238 (0.0864,0.9894)	9.7749 (2.4480,14.5379)
	0.5721 (0.1000,1.9027)	3.4526 (0.8596,4.9960)	0.0612 (3.52E-08,0.2293)	0.8486 (0.2387,1.0000)	0.4567 (0.0229,0.9789)	9.7798 (2.3262,14.5157)
16	0.2658 (0.1000,1.4845)	2.7361 (0.6207,4.9426)	0.4624 (0.1359,0.7584)	0.8106 (0.3348,0.9995)	0.6293 (0.0647,0.9928)	7.3939 (1.7679,14.9236)
	0.3275 (0.1000,1.7543)	3.0032 (0.7106,4.9465)	0.3792 (0.1088,0.6881)	0.8035 (0.2279,0.9998)	0.5700 (0.0805,0.9653)	8.0892 (1.7505,14.1970)

Table 12 Confidence intervals for estimated parameters. Same information as Table 11 but obtained by MCMC method

Region	α mean 95%CI	β_0 mean 95%CI	$\rho_{s,1}$ mean 95%CI	$\rho_{s,2}$ mean 95%CI	q_β mean 95%CI	R_0 mean 95%CI
1	0.6154 (0.1000,1.9001)	2.0897 (0.5735,4.9969)	0.3127 (5.38E-05,0.9959)	0.7696 (0.1261,1.0000)	0.0922 (9.98E-07,0.4667)	5.8229 (1.7523,14.5437)
	0.6905 (0.1000,1.9949)	2.8356 (0.6295,4.9994)	0.2050 (1.88E-06,0.9975)	0.7345 (0.1602,0.9999)	0.1227 (9.17E-07,0.4732)	7.7677 (1.8254,14.5471)
2	0.5981 (0.1000,1.7125)	3.5688 (0.4250,4.9984)	0.2915 (0.0005,0.9987)	0.7240 (0.0618,0.9999)	0.1655 (0.0010,0.7117)	9.3002 (1.5444,15.2575)
	0.8217 (0.1002,1.9990)	3.6308 (0.7103,5.0000)	0.1564 (1.36E-06,0.9994)	0.8058 (0.0174,1.0000)	0.2518 (0.0005,0.6369)	10.1497 (1.3699,14.5616)
3	0.7436 (0.1018,1.9997)	2.4670 (0.5645,4.9998)	0.4576 (0.0009,1.0000)	0.5092 (0.0021,0.9996)	0.0932 (0.0002,0.3780)	6.7190 (1.5141,15.8481)
	1.1940 (0.1004,1.9999)	3.2414 (0.6962,5.0000)	0.2622 (0.0002,0.8437)	0.7191 (0.1856,0.9998)	0.1567 (0.0005,0.6391)	8.4040 (1.5237,14.5507)
4	0.8472 (0.1000,1.9982)	1.8162 (0.5895,4.9989)	0.5112 (1.12E-05,1.0000)	0.5474 (0.0281,1.0000)	0.1190 (5.98E-07,0.9987)	4.5161 (1.3153,14.5448)
	1.0722 (0.1002,1.9995)	1.6972 (0.5008,4.9978)	0.4895 (0.0002,1.0000)	0.7034 (0.2363,0.9998)	0.0928 (6.06E-07,0.8073)	3.8354 (1.3778,14.5382)
5	0.4626 (0.1000,1.9972)	3.7554 (0.4593,5.0000)	0.1883 (1.0E-06,0.9816)	0.6223 (0.0612,1.0000)	0.0910 (6.00E-07,0.5282)	10.2696 (1.3784,17.5936)
	0.7097 (0.1000,1.9980)	2.3500 (0.4307,4.9991)	0.2425 (1.72E-06,0.9977)	0.6888 (0.0508,1.0000)	0.0562 (4.26E-07,0.4547)	6.2828 (1.3516,14.7540)
6	0.8887 (0.1001,1.9994)	3.4641 (0.5667,4.9993)	0.1220 (1.63E-06,0.9987)	0.8072 (0.1118,1.0000)	0.4584 (0.0005,0.9997)	9.7700 (1.5879,14.5537)
	0.9409 (0.1002,1.9999)	3.3338 (0.5325,4.9990)	0.1188 (9.68E-06,0.9968)	0.8082 (0.1848,1.0000)	0.4518 (6.86E-05,0.9997)	9.2606 (1.3773,14.5560)
7	0.5150 (0.1000,1.7571)	2.8975 (0.4047,5.0000)	0.1656 (0.0005,0.9969)	0.5253 (0.1538,0.9999)	0.1898 (7.18E-07,0.6143)	8.2062 (1.2628,14.6380)
	0.3919 (0.1000,1.3052)	2.1112 (0.5682,4.9992)	0.4983 (5.06E-05,0.9998)	0.6405 (0.2085,1.0000)	0.1180 (1.17E-06,0.5510)	5.4909 (1.5671,14.5540)
8	0.3212 (0.1000,1.9782)	2.4211 (0.4387,4.9984)	0.5270 (0.1010,0.9997)	0.9191 (0.5125,1.0000)	0.2443 (1.63E-06,0.9980)	6.7118 (1.2270,15.5378)
	0.2892 (0.1000,1.2950)	4.3716 (1.6107,5.0000)	0.1851 (0.0555,0.3852)	0.9489 (0.6058,1.0000)	0.5199 (0.1848,0.9995)	12.5786 (4.8208,15.2979)
9	0.1061 (0.1000,0.1994)	3.9914 (1.5666,4.9996)	0.7567 (0.2485,0.9997)	0.6845 (0.2767,0.9999)	0.6532 (0.2562,1.0000)	13.8279 (5.6350,18.7700)
	0.1091 (0.1000,0.1098)	1.8115 (1.4024,2.1588)	0.2599 (0.0774,0.4302)	0.8470 (0.3769,0.9986)	0.0014 (2.90E-07,0.0040)	5.6240 (4.5335,6.8430)
10	0.2209 (0.1000,0.8291)	4.2283 (2.3492,4.9994)	0.8042 (0.4855,1.0000)	0.7939 (0.4150,1.0000)	0.6196 (0.1760,0.9995)	14.0333 (8.3162,18.9913)
	0.1089 (0.1000,0.1669)	4.2591 (2.6027,5.0000)	0.6905 (0.4133,0.9996)	0.9401 (0.4797,1.0000)	0.5099 (0.2635,0.9983)	14.3664 (8.6457,18.5251)
11	0.5398 (0.1000,1.9967)	2.9427 (0.0015,4.9995)	0.4622 (0.1838,0.8332)	0.8736 (0.4526,1.0000)	0.7952 (0.0008,1.0000)	7.4681 (0.0044,16.1540)
	0.6652 (0.1000,1.9990)	1.9363 (0.0004,4.9983)	0.4032 (0.1992,0.7627)	0.8289 (0.4616,1.0000)	0.3698 (4.78E-07,0.9996)	5.4179 (0.0009,13.8172)
12	0.2105 (0.1000,0.8362)	3.4912 (0.5473,5.0000)	0.5352 (0.1784,0.9993)	0.6989 (0.1605,0.9999)	0.0048 (1.56E-06,0.0631)	10.4372 (1.9273,18.9652)
	0.1380 (0.1000,0.4566)	3.5342 (1.9954,5.0000)	0.4250 (0.0796,0.9995)	0.9225 (0.6224,1.0000)	0.0015 (1.85E-07,0.0042)	11.3471 (5.0611,18.8555)
13	0.8622 (0.1007,1.9201)	2.0179 (0.8341,4.9927)	0.7143 (2.21E-06,1.0000)	0.8620 (0.5222,1.0000)	0.0081 (0.0001,0.0929)	4.1329 (1.7918,14.5297)
	0.3513 (0.1000,0.9107)	3.2895 (1.1821,5.0000)	0.0343 (1.48E-06,0.1084)	0.5472 (0.1111,0.9997)	0.0080 (5.64E-07,0.1057)	9.5085 (3.2350,14.5576)
14	0.1160 (0.1000,0.2519)	1.6161 (0.0006,4.9910)	0.6817 (0.2053,0.9998)	0.8669 (0.4667,1.0000)	0.7833 (0.2561,1.0000)	5.2602 (0.0020,16.8316)
	0.3209 (0.1000,1.6305)	3.3242 (0.0075,5.0000)	0.5245 (0.1001,0.9993)	0.8291 (0.3438,1.0000)	0.7223 (0.3123,0.9999)	9.4291 (0.0255,17.2904)
15	0.3119 (0.1000,1.7127)	3.8879 (0.8507,5.0000)	0.3486 (0.0028,0.8292)	0.8400 (0.3074,1.0000)	0.4606 (0.1501,0.9996)	11.4818 (2.5682,17.7744)
	0.6332 (0.1000,1.9987)	2.2246 (0.6387,4.9964)	0.7822 (0.1348,1.0000)	0.6194 (0.3915,1.0000)	0.1450 (3.23E-05,0.9992)	5.6244 (1.3749,18.3794)
16	0.1386 (0.1000,0.6439)	2.1958 (0.0012,5.0000)	0.7261 (0.0017,1.0000)	0.8061 (0.2524,1.0000)	0.7512 (0.0015,1.0000)	6.7164 (0.0043,16.9113)
	0.2179 (0.1000,1.1764)	2.8257 (0.0027,4.9997)	0.6984 (0.1255,1.0000)	0.8338 (0.2245,1.0000)	0.7027 (0.1898,0.9999)	8.4036 (0.0099,18.7511)

Table 13 Confidence intervals for parameters $J(0)$,$I_s(0)$, p_1, p_2, p_3 and p_4 estimated using SA method. For each region the estimates are computed using cases reported of symptomatic and asymptomatic (first row per region), and symptomatic, asymptomatic, and without-notifying (second row per region) individuals, based on regional data from Chile

Region	$J(0)$ mean 95%CI	$I_s(0)$ mean 95% IC	p_1 mean 95%CI	p_2 mean 95%CI	p_3 mean 95%CI	p_4 mean 95%CI
1	0.5200 (0.0079,0.9927)	224.2537 (65.8896,295.0683)	0.0062 (2.25E-14,0.0240)			
	0.4876 (0.0098,0.9827)	206.4261 (40.6093,295.6976)	0.0172 (5.55E-11,0.0947)			
2	0.9905 (0.0310,1.9886)	219.7943 (49.9773,299.2569)	0.0033 (3.99E-14,0.0383)	0.4503 (0.0017,0.9916)	0.4817 (0.0115,0.9860)	
	1.0060 (0.0291,1.9821)	245.1751 (116.4945,299.5314)	0.0027 (4.29E-11,0.0276)	0.4662 (0.0227,0.9732)	0.4931 (0.0076,0.9927)	
3	0.5823 (0.0279,0.9988)	13.3635 (2.0586,28.6212)				
	0.5301 (0.0184,0.9908)	30.6178 (9.3713,47.1285)				
4	1.1061 (0.0420,1.9995)	60.1332 (14.4596,145.7553)				
	1.0970 (0.0366,1.9879)	152.2432 (84.5459,205.5763)				
5	0.5094 (0.0135,0.9770)	216.8185 (42.1728,299.4247)	0.2578 (2.76E-14,0.8477)	0.4521 (0.0017,0.9754)	0.5336 (0.0123,0.9904)	
	0.4852 (0.0036,0.9937)	225.8146 (58.8992,299.4745)	0.2242 (4.02E-09,0.8060)	0.4042 (0.0031,0.9764)	0.5385 (0.0161,0.9895)	
6	0.9423 (0.0456,1.9404)	146.5750 (73.6642,218.3597)	0.4999 (0.0103,0.9909)			
	1.0200 (0.0539,1.9744)	170.0988 (73.0872,257.9385)	0.4912 (0.0100,0.9899)			
7	0.5422 (0.0107,0.9855)	178.0730 (107.3993,235.8145)	0.4802 (0.0118,0.9806)			
	0.5150 (0.0404,0.9819)	165.8868 (102.5833,217.2181)	0.4976 (0.0093,0.9876)			
8	0.4911 (0.0056,0.9823)	217.8191 (80.9032,298.2846)	0.0025 (5.06E-20,0.0272)			
	0.5124 (0.0160,0.9933)	192.8313 (96.2252,295.5741)	0.0039 (1.41E-10,0.0330)			
9	0.4881 (0.0130,0.9973)	151.6382 (5.0668,297.0497)	0.5484 (0.0004,0.9918)	0.5357 (0.0002,0.9909)	0.4259 (1.02E-05,0.9838)	0.3105 (0.0005,0.9671)
	0.4956 (0.0087,0.9959)	177.7536 (17.5667,298.6403)	0.6153 (0.0001,0.9957)	0.4812 (8.66E-06,0.9885)	0.4002 (8.65E-06,0.9792)	0.2875 (5.90E-05,0.9715)
10	0.5265 (0.0068,0.9939)	117.9256 (39.6034,221.0185)	0.0169 (4.89E-09,0.0662)			
	0.5074 (0.0096,0.9731)	151.0274 (63.4453,265.9032)	0.0050 (1.15E-10,0.0182)			
11	0.5652 (0.0132,0.9855)	1.3305 (0.0044,4.8793)	0.0285 (3.42E-14,0.3688)			
	0.6238 (0.0336,0.9938)	1.3254 (0.0091,5.0794)	0.0849 (1.68E-14,0.9573)			
12	0.9847 (0.0159,1.9812)	100.8092 (5.2962,247.5471)	0.3620 (2.64E-05,0.9702)	0.3579 (4.82E-05,0.9902)		
	1.0277 (0.0179,1.9938)	221.8528 (99.6702,299.8017)	0.1313 (1.13E-07,0.9419)	0.0314 (2.63E-14,0.4656)		
13	0.5164 (0.0067,0.9929)	166.2956 (8.0433,296.5386)	0.2857 (0.0001,0.5467)	0.0883 (2.90E-05,0.6820)	0.5145 (0.0180,0.9969)	0.4930 (0.0065,0.9923)
	0.4869 (0.0065,0.9924)	148.3297 (5.6401,297.2723)	0.3273 (4.02E-05,0.8158)	0.0450 (6.60E-06,0.4340)	0.5126 (0.0066,0.9955)	0.4947 (0.0047,0.9919)
14	0.4918 (0.0261,0.9665)	60.1428 (25.1453,109.7113)				
	0.5298 (0.0258,0.9859)	83.7939 (33.4655,141.5601)				
15	0.5124 (0.0060,0.9927)	131.3704 (67.0047,199.6104)	0.0003 (4.33E-14,0.0025)			
	0.4951 (0.0038,0.9981)	108.0327 (36.7021,187.9724)	0.0014 (6.91E-10,0.0091)			
16	0.5102 (0.0252,0.9860)	196.5099 (87.2325,297.0178)	0.0045 (5.19E-11,0.0081)			
	0.5129 (0.0241,0.9889)	197.9070 (98.8915,298.9420)	0.0015 (2.26E-11,0.0120)			

Table 14 Confidence intervals for estimated parameters. Same information as Table 13 but obtained by MCMC method

Region	$J(0)$ mean 95%CI	$I_s(0)$ mean 95% IC	p_1 mean 95%CI	p_2 mean 95%CI	p_3 mean 95%CI	p_4 mean 95%CI
1	0.5627 (2.29E-06,1.0000)	69.9225 (0.1642,299.7127)	0.0326 (3.28E-06,0.1086)			
	0.6394 (0.0010,0.9999)	83.1887 (0.0003,299.5650)	0.1343 (5.22E-07,0.9435)			
2	1.1769 (0.0009,2.0000)	84.6234 (0.0002,299.9012)	0.0390 (6.85E-07,0.7661)	0.7172 (3.59E-04,1.0000)	0.7111 (0.0002,1.0000)	
	0.8847 (3.68E-06,1.9992)	199.3934 (0.1202,299.9493)	0.0245 (6.76E-07,0.2574)	0.4760 (1.99E-06,0.9997)	0.5006 (0.0001,0.9999)	
3	0.6012 (0.0003,0.9993)	2.4217 (0.0284,23.6564)				
	0.5653 (0.0008,0.9998)	6.2105 (0.0002,35.7107)				
4	1.0239 (6.53E-06,1.9992)	21.0928 (0.0158,114.1688)				
	1.2781 (0.0002,1.9999)	16.2948 (0.0002,112.6781)				
5	0.4423 (1.47E-06,0.9999)	154.2947 (0.1647,299.9745)	0.2231 (2.22E-07,0.8042)	0.5673 (3.05E-04,0.9997)	0.4573 (1.20E-06,1.0000)	
	0.6489 (0.0001,0.9999)	193.8629 (0.1223,299.9282)	0.1214 (3.39E-07,0.7419)	0.5380 (2.35E-06,0.9996)	0.3726 (1.74E-06,0.9998)	
6	1.0482 (0.0003,1.9998)	89.3021 (0.0477,208.8540)	0.5377 (2.66E-04,0.9999)			
	1.1759 (0.0008,1.9997)	107.2947 (0.1684,272.4032)	0.5440 (0.0002,1.0000)			
7	0.4955 (1.30E-06,0.9995)	120.3018 (35.2232,223.7701)	0.3920 (6.37E-05,0.9998)			
	0.7650 (0.0003,1.0000)	51.9775 (0.0002,225.7289)	0.6776 (0.0004,0.9995)			
8	0.4181 (0.0005,0.9997)	130.2732 (21.6757,299.6667)	0.0026 (4.77E-07,0.0058)			
	0.4866 (0.0002,0.9997)	200.6713 (51.5523,299.9395)	0.0025 (7.00E-07,0.0153)			
9	0.5603 (0.0002,1.0000)	206.9838 (88.4983,299.9651)	0.0292 (8.50E-07,0.2764)	0.0025 (5.85E-07,0.0124)	0.0723 (5.42E-07,0.7229)	0.4000 (6.28E-05,0.9997)
	0.2099 (0.0001,0.9053)	173.5552 (82.7871,296.2257)	0.7263 (0.3903,0.9999)	0.8739 (0.4634,1.0000)	0.2751 (0.0010,0.5087)	0.2776 (3.93E-06,0.9983)
10	0.3256 (1.46E-06,0.9993)	50.4576 (22.1976,93.2962)	0.0026 (7.44E-07,0.0060)			
	0.5046 (0.0008,1.0000)	49.2407 (17.9215,98.3712)	0.0021 (8.11E-07,0.0057)			
11	0.5502 (0.0005,1.0000)	0.6487 (0.0004,2.3827)	0.0320 (4.16E-07,0.5959)			
	0.7370 (0.1860,0.9998)	0.4897 (0.0002,1.3169)	0.1685 (7.19E-07,0.6135)			
12	1.0637 (0.1822,1.9987)	31.2680 (0.0238,146.1991)	0.3930 (2.69E-06,0.9997)	0.4413 (0.0467,0.9952)		
	0.5853 (2.49E-06,2.0000)	37.5446 (0.0007,112.8554)	0.3808 (3.13E-06,1.0000)	0.6835 (0.2875,0.9997)		
) 13	0.2230 (0.0002,0.9969)	238.5443 (18.6493,299.9925)	0.0504 (6.27E-07,0.4542)	0.0394 (3.88E-06,0.1060)	0.7969 (0.0007,1.0000)	0.2801 (1.52E-06,0.9993)
	0.3590 (1.22E-06,0.9994)	123.0193 (2.0101,299.9994)	0.1612 (0.0003,0.5067)	0.0687 (5.13E-07,0.1720)	0.8522 (0.0008,1.0000)	0.3423 (1.33E-06,0.9981)
14	0.7300 (0.0008,1.0000)	60.6757 (17.9316,100.4363)				
	0.4542 (4.69E-05,1.0000)	52.2764 (21.3049,105.4026)				
15	0.3623 (0.0002,0.9995)	62.6027 (0.2560,158.3092)	0.0021 (7.05E-07,0.0074)			
	0.8667 (0.0096,0.9995)	35.0948 (0.0003,127.1882)	0.0085 (6.67E-07,0.0584)			
16	0.4691 (0.0002,0.9996)	214.3314 (75.0893,299.9997)	0.0400 (8.57E-07,0.7274)			
	0.4409 (1.27E-06,0.9999)	183.0261 (56.4767,299.9712)	0.0015 (8.00E-07,0.0046)			

Table 15 Sensitivity indices for R_0 obtained for parameters estimated using SA method. For each region the estimates are computed using cases reported of symptomatic and asymptomatic (first row per region), and symptomatic, asymptomatic, and without-notifying (second row per region) individuals, based on regional data from Chile

Region	$\Gamma_{\beta}^{R_0}$	$\Gamma_{h}^{R_0}$	$\Gamma_{q_{\mathrm{e}}}^{R_0}$	$\Gamma_{q_{\mathrm{a}}}^{R_0}$	$\Gamma_{q}^{R_0}$	$\Gamma_{\kappa 2}^{R_0}$	$\Gamma_{\rho_{\mathrm{a}}}^{R_0}$	$\Gamma_{\rho_{\mathrm{s}}}^{R_0}$	$\Gamma_{\alpha}^{R_0}$	$\Gamma_{\gamma_1}^{R_0}$	$\Gamma_{\gamma_2}^{R_0}$	$\Gamma_{\delta}^{R_0}$
1	1.0000	0.0000	0.8216	0.0376	0.1784	-0.8216	-0.0563	1.04E-05	-1.06E-05	-0.1784	0.0000	0.0000
	1.0000	0.0000	0.7616	0.0348	0.2384	-0.7616	-0.1009	7.30E-02	-7.74E-02	-0.1610	0.0000	0.0000
2	1.0000	0.0000	0.6006	0.0275	0.3994	-0.6006	-0.2205	0.2690	-0.3714	-0.0280	0.0000	0.0000
	1.0000	0.0000	0.7205	0.0329	0.2795	-0.7205	-0.1315	0.1231	-0.1282	-0.1513	0.0000	0.0000
3	1.0000	0.0000	0.4873	0.0223	0.5127	-0.4873	-0.3047	0.4069	-0.4128	-0.0999	0.0000	0.0000
	1.0000	0.0000	0.8216	0.0376	0.1784	-0.8216	-0.0563	8.19E-11	-9.67E-11	-0.1784	0.0000	0.0000
4	1.0000	0.0000	0.7871	0.0360	0.2129	-0.7871	-0.0820	0.0420	-0.0480	-0.1649	0.0000	0.0000
	1.0000	0.0000	0.8216	0.0376	0.1784	-0.8216	-0.0563	1.03E-07	-1.05E-07	-0.1784	0.0000	0.0000
5	1.0000	0.0000	0.7750	0.0354	0.2250	-0.7750	-0.0910	0.0568	-0.0576	-0.1675	0.0000	0.0000
	1.0000	0.0000	0.7496	0.0343	0.2504	-0.7496	-0.1098	0.0876	-0.0889	-0.1615	0.0000	0.0000
6	1.0000	0.0000	0.8216	0.0376	0.1784	-0.8216	-0.0563	9.04E-12	-9.30E-12	-0.1784	0.0000	0.0000
	1.0000	0.0000	0.8216	0.0376	0.1784	-0.8216	-0.0563	4.36E-09	-4.43E-09	-0.1784	0.0000	0.0000
7	1.0000	0.0000	0.8114	0.0371	0.1886	-0.8114	-0.0639	0.0124	-0.0126	-0.1760	0.0000	0.0000
	1.0000	0.0000	0.7882	0.0360	0.2118	-0.7882	-0.0811	0.0406	-0.0416	-0.1701	0.0000	0.0000
8	1.0000	0.0000	0.7769	0.0355	0.2231	-0.7769	-0.0896	0.0544	-0.0584	-0.1648	0.0000	0.0000
	1.0000	0.0000	0.5727	0.0262	0.4273	-0.5727	-0.2413	0.3030	-0.3082	-0.1191	0.0000	0.0000
9	1.0000	0.0000	0.4549	0.0208	0.5451	-0.4549	-0.3288	0.4464	-0.4572	-0.0879	0.0000	0.0000
	1.0000	0.0000	0.7039	0.0322	0.2961	-0.7039	-0.1437	0.1432	-0.1813	-0.1148	0.0000	0.0000
10	1.0000	0.0000	0.0812	0.0037	0.9188	-0.0812	-0.6064	0.9012	-0.9142	-0.0046	0.0000	0.0000
	1.0000	0.0000	0.2152	0.0098	0.7848	-0.2152	-0.5068	0.7380	-0.7487	-0.0360	0.0000	0.0000
11	1.0000	0.0000	0.6895	0.0315	0.3105	-0.6895	-0.1544	0.1607	-0.2028	-0.1077	0.0000	0.0000
	1.0000	0.0000	0.3165	0.0145	0.6835	-0.3165	-0.4315	0.6148	-0.6237	-0.0598	0.0000	0.0000
12	1.0000	0.0000	0.6331	0.0289	0.3669	-0.6331	-0.1963	0.2294	-0.2372	-0.1297	0.0000	0.0000
	1.0000	0.0000	0.1047	0.0048	0.8953	-0.1047	-0.5889	0.8725	-0.8852	-0.0101	0.0000	0.0000
13	1.0000	0.0000	0.8214	0.0375	0.1786	-0.8214	-0.0565	0.0003	-0.0003	-0.1783	0.0000	0.0000
	1.0000	0.0000	0.7655	0.0350	0.2345	-0.7655	-0.0980	0.0683	-0.0696	-0.1649	0.0000	0.0000
14	1.0000	0.0000	0.2985	0.0136	0.7015	-0.2985	-0.4449	0.6367	-0.6459	-0.0556	0.0000	0.0000
	1.0000	0.0000	0.5056	0.0231	0.4944	-0.5056	-0.2911	0.3846	-0.3901	-0.1042	0.0000	0.0000
15	1.0000	0.0000	0.6604	0.0302	0.3396	-0.6604	-0.1761	0.1962	-0.1994	-0.1403	0.0000	0.0000
	1.0000	0.0000	0.4300	0.0197	0.5700	-0.4300	-0.3472	0.4766	-0.4906	-0.0794	0.0000	0.0000
16	1.0000	0.0000	0.1491	0.0068	0.8509	-0.1491	-0.5559	0.8185	-0.8329	-0.0180	0.0000	0.0000
	1.0000	0.0000	0.2121	0.0097	0.7879	-0.2121	-0.5091	0.7418	-0.7545	-0.0334	0.0000	0.0000

Table 16 Sensitivity indices for R_0. Same information as in Table 15 but obtained by using MCMC.

Region	$\Gamma_{\beta}^{R_0}$	$\Gamma_{h}^{R_0}$	$\Gamma_{q_{\mathrm{e}}}^{R_0}$	$\Gamma_{q_{\mathrm{a}}}^{R_0}$	$\Gamma_{q}^{R_0}$	$\Gamma_{\kappa_2}^{R_0}$	$\Gamma_{\rho_{\mathrm{a}}}^{R_0}$	$\Gamma_{\rho_{s}}^{R_0}$	$\Gamma_{\alpha}^{R_0}$	$\Gamma_{\gamma_1}^{R_0}$	$\Gamma_{\gamma_2}^{R_0}$	$\Gamma_{\delta}^{R_0}$
1	1.0000	0.0000	0.0870	0.0040	0.9130	-0.0870	-0.6021	0.8942	-0.9071	-0.0059	0.0000	0.0000
	1.0000	0.0000	0.6305	0.0288	0.3695	-0.6305	-0.1983	0.2326	-0.3227	-0.0468	0.0000	0.0000
2	1.0000	0.0000	0.6818	0.0312	0.3182	-0.6818	-0.1602	0.1702	-0.1726	-0.1456	0.0000	0.0000
	1.0000	0.0000	0.4266	0.0195	0.5734	-0.4266	-0.3498	0.4807	-0.4881	-0.0853	0.0000	0.0000
3	1.0000	0.0000	0.2965	0.0136	0.7035	-0.2965	-0.4464	0.6391	-0.6489	-0.0546	0.0000	0.0000
	1.0000	0.0000	0.6915	0.0316	0.3085	-0.6915	-0.1530	0.1584	-0.2091	-0.0994	0.0000	0.0000
4	1.0000	0.0000	0.6073	0.0278	0.3927	-0.6073	-0.2155	0.2608	-0.3649	-0.0278	0.0000	0.0000
	1.0000	0.0000	0.4188	0.0191	0.5812	-0.4188	-0.3555	0.4902	-0.5619	-0.0192	0.0000	0.0000
5	1.0000	0.0000	0.5587	0.0255	0.4413	-0.5587	-0.2516	0.3200	-0.3843	-0.0571	0.0000	0.0000
	1.0000	0.0000	0.6031	0.0276	0.3969	-0.6031	-0.2186	0.2659	-0.3302	-0.0667	0.0000	0.0000
6	1.0000	0.0000	0.2044	0.0093	0.7956	-0.2044	-0.5148	0.7512	-0.7863	-0.0094	0.0000	0.0000
	1.0000	0.0000	0.2861	0.0131	0.7139	-0.2861	-0.4541	0.6517	-0.6831	-0.0307	0.0000	0.0000
7	1.0000	0.0000	0.4618	0.0211	0.5382	-0.4618	-0.3236	0.4379	-0.5169	-0.0213	0.0000	0.0000
	1.0000	0.0000	0.1590	0.0073	0.8410	-0.1590	-0.5486	0.8065	-0.8202	-0.0208	0.0000	0.0000
8	1.0000	0.0000	0.1395	0.0064	0.8605	-0.1395	-0.5630	0.8302	-0.8426	-0.0178	0.0000	0.0000
	1.0000	0.0000	0.3900	0.0178	0.6100	-0.3900	-0.3770	0.5254	-0.5332	-0.0768	0.0000	0.0000
9	1.0000	0.0000	0.1176	0.0054	0.8824	-0.1176	-0.5793	0.8569	-0.8699	-0.0125	0.0000	0.0000
	1.0000	0.0000	0.1780	0.0081	0.8220	-0.1780	-0.5345	0.7834	-0.7949	-0.0272	0.0000	0.0000
10	1.0000	0.0000	0.5230	0.0239	0.4770	-0.5230	-0.2782	0.3635	-0.4120	-0.0651	0.0000	0.0000
	1.0000	0.0000	0.1266	0.0058	0.8734	-0.1266	-0.5726	0.8459	-0.8594	-0.0140	0.0000	0.0000
11	1.0000	0.0000	0.2535	0.0116	0.7465	-0.2535	-0.4784	0.6915	-0.7022	-0.0443	0.0000	0.0000
	1.0000	0.0000	0.4970	0.0227	0.5030	-0.4970	-0.2975	0.3951	-0.4600	-0.0430	0.0000	0.0000
12	1.0000	0.0000	0.0770	0.0035	0.9230	-0.0770	-0.6095	0.9063	-0.9195	-0.0035	0.0000	0.0000
	1.0000	0.0000	0.1227	0.0056	0.8773	-0.1227	-0.5755	0.8507	-0.8638	-0.0135	0.0000	0.0000
13	1.0000	0.0000	0.5600	0.0256	0.4400	-0.5600	-0.2507	0.3184	-0.4142	-0.0258	0.0000	0.0000
	1.0000	0.0000	0.7970	0.0364	0.2030	-0.7970	-0.0746	0.0300	-0.0304	-0.1726	0.0000	0.0000
14	1.0000	0.0000	0.1879	0.0086	0.8121	-0.1879	-0.5271	0.7713	-0.7825	-0.0296	0.0000	0.0000
	1.0000	0.0000	0.3599	0.0165	0.6401	-0.3599	-0.3993	0.5620	-0.5704	-0.0697	0.0000	0.0000
15	1.0000	0.0000	0.1594	0.0073	0.8406	-0.1594	-0.5483	0.8060	-0.8177	-0.0229	0.0000	0.0000
	1.0000	0.0000	0.5434	0.0248	0.4566	-0.5434	-0.2630	0.3386	-0.4167	-0.0399	0.0000	0.0000
16	1.0000	0.0000	0.1701	0.0078	0.8299	-0.1701	-0.5403	0.7930	-0.8047	-0.0252	0.0000	0.0000
	1.0000	0.0000	0.2033	0.0093	0.7967	-0.2033	-0.5157	0.7526	-0.7637	-0.0330	0.0000	0.0000

References

1. World Health Organization. WHO Director-General's opening remarks at the media briefing on COVID-19-11 March 2020 World Health Organization 2020 [April 23]. Available from: https://bit.ly/ 2A8aCIO.
2. Chan JF-W, Yuan S, Kok K-H, To KK-W, Chu H, Yang J, et al. A familial cluster of pneumonia associ- ated with the 2019 novel coronavirus indicating person-to-person transmission: a study of a family cluster. Lancet 2020;395(10223):514–23. https://doi.org/10.1016/S0140-6736(20)30154-9
3. Li Y, Campbell H, Kulkarni D, Harpur A, Nundy M, Wang X, et al. The temporal association of introducing and lifting non-pharmaceutical interventions with the time-varying reproduction number (R) of SARS-CoV-2: a modelling study across 131 countries. Lancet Infect Dis. 2020:Epub October 22. https://doi.org/10.1016/S1473-3099(20)30785-4
4. Walker PGT, Whittaker C, Watson OJ, Baguelin M, Winskill P, Hamlet A, et al. The impact of COVID-19 and strategies for mitigation and suppression in low- and middle-income countries. Science (New York, NY) 2020;369(6502):413–22. https://doi.org/10.1126/science.abc0035
5. Flaxman S, Mishra S, Gandy A, Unwin HJT, Mellan TA, Coupland H, et al. Estimating the effects of non-pharmaceutical interventions on COVID-19 in Europe. Nature 2020;584(7820):257–61. https:// doi.org/10.1038/s41586-020-2405-7
6. Burki T. COVID-19 in Latin America. Lancet Infect Dis. 2020;20(5):547–8.
7. Garcia PJ, Alarcón A, Bayer A, Buss P, Guerra G, Ribeiro H, et al. COVID-19 response in Latin America. Am J Trop Med Hyg. 2020;103(5):1765–72.
8. Navarro JC, Arrivillaga-Henríquez J, Salazar-Loor J, Rodriguez-Morales AJ. COVID-19 and dengue, co-epidemics in Ecuador and other countries in Latin America: pushing strained health care systems over the edge. Travel Med Infect Dis. 2020;37:101656.
9. Kirby T. South America prepares for the impact of COVID-19. Lancet Respir Med. 2020;8(6):551–2.
10. Ministerio de Salud, Chile http://www.minsal.cl (accessed February 15, 2021).
11. Undurraga EA, Chowell G, Mizumoto K. COVID-19 case fatality risk by age and gender in a high testing setting in Latin America: Chile, March–August 2020. Infect Dis Poverty 2021;10:11. https://doi.org/10.1186/s40249-020-00785-1
12. The Conversation: How Chile became an unlikely winner in the COVID-19 vaccine race (February 10, 2021). https://theconversation.com/how-chile-became-an-unlikely-winner-in-the-covid-19-vaccine-race-154614 (accessed February 15, 2021).
13. Anderson RM, May RM. Infectious diseases of humans: dynamics and control. Oxford: Oxford Science Publications; 1991.
14. Vynnycky E, White RE. An introduction to infectious disease modelling. Oxford: Oxford University Press; 2010.
15. Brauer F, Castillo-Chavez C. Mathematical models in population biology and epidemiology. 2nd ed. New York: Springer; 2012.
16. Diekmann O, Heesterbeek H, Britton T. Mathematical tools for understanding infectious disease dynamics. Princeton: Princeton University Press; 2012.
17. Martcheva M. An introduction to mathematical epidemiology. New York: Springer; 2015.
18. Yan P, Chowell G. Quantitative methods for investigating infectious disease outbreaks. Cham, Switzerland: Springer; 2019.
19. Kermack WO, McKendrick AG. A contribution to the mathematical theory of epidemics. Proc Roy Soc A. 1927;115:700–21.
20. Wang XS, Wu J, Yang Y. Richards model revisited: validation by and application to infection dynamics. J Theor Biol. 2012;313:12–9.
21. Chowell G, Sattenspiel L, Bansal S, Viboud C. Mathematical models to characterize early epidemic growth. A review. Phys Life Rev. 2016;18:66–97. doi: https://doi.org/10.1016/j.plrev.2016.07.005
22. Chowell G, Viboud C, Simonsen L, Moghadas SM. Characterizing the reproduction number of epidemics with early subexponential growth dynamics. J R Soc Interface 2016;13:0659. doi: https://doi.org/10.1098/rsfit.2016.0659
23. Chowell G, Hincapie-Palacio D, Ospina J, Pell B, Tariq A, Dahal S, Moghadas S, Smirnova A, Simonsen L, Viboud C. Using phenomenological models to characterize transmissibility and forecast patterns and final burden of Zika epidemics. PLoS Currents Outbreaks 2016 (Ed. 1, 31 May). doi: 10.1371/currents.outbreaks.f14b2217c902f453d9320a43a35b9583

24. Pell B, Kuang Y, Viboud C, Chowell G. Using phenomenological models for forecasting the 2015 Ebola challenge. Epidemics 2018;22:62–70.
25. Bürger R, Chowell G, Lara-Díaz LY. Comparative analysis of phenomenological growth models applied to epidemic outbreaks. Math Biosci Eng. 2019;16:4250–73.
26. Bürger R, Chowell G, Lara-Díaz LY. Measuring differences between phenomenological growth models applied to epidemiology. Math Biosci. 2021;334:108558. https://doi.org/10.1016/j.mbs.2021.108558.
27. Metropolis N, Rosenbluth AW, Rosenbluth MN, Teller AH, Teller E. Equation of state calculations by fast computing machines. J Chem Phys. 1953;21:1087–92, https://doi.org/10.1063/1.1699114
28. Hastings WK. Monte Carlo sampling methods using Markov chains and their applications. Biometrika 1970:57,97–109.
29. Vidal RVV (Ed). Applied simulated annealing. Lecture Notes in Economics and Mathematical Systems. Berlin: Springer-Verlag; 1993.
30. Brooks SP, Morgan BJT. Optimization using simulated annealing, J Roy Stat Soc Ser D (The Statistician) 1995;44:241–57.
31. Abbasi B, Jahromi AHE, Arkat J, Hosseinkouchack M. Estimating the parameters of Weibull distribution using simulated annealing algorithm. Appl Math Comput. 2006;183:85–93.
32. Chuine I, Cour P, Rousseau DD. Fitting models predicting dates of flowering of temperate-zone trees using simulated annealing. Plant, Cell & Environment 1998;21:455–66.
33. Spall JC. Estimation via Markov chain Monte Carlo. IEEE Control Syst Mag. 2003;23(2):34–45.
34. Berg BA. Markov chain Monte Carlo simulations and their statistical analysis. Singapore: World Scientific; 2004.
35. Asmussen S, Glynn PW. Stochastic simulation: algorithms and analysis. New York: Springer-Verlag; 2007.
36. Rubinstein RY, Kroese DP. Simulation and the Monte Carlo method. Hoboken, NJ: Wiley; 2017.
37. Hill SD, Spall JC. Stationarity and convergence of the Metropolis-Hastings algorithm: insights into theoretical aspects. IEEE Control Systems Magazine 2019;39(1):56–67.
38. Chowell G, Chowell D, Roosa K, Dhillon R, Devabhaktuni S. Sustainable social distancing through facemask use and testing during the Covid-19 pandemic. Preprint, medRXiv; 2020. doi: https://doi.org/10.1101/2020.04.01.20049981
39. Jia J, Ding J, Liu S, Liao G, Li J, Duan B, Wang G, Zhang R. Modeling the control of COVID-19: impact of policy interventions and meteorological factors. Electron J Differ Equations. 2020;2020(23):1–24.
40. Peng, L., et al., Epidemic analysis of COVID-19 in China by dynamical modeling, medRxiv 2020, doi: https://doi.org/10.1101/2020.02.16.20023465
41. Castilho C, Gondim JAM, Marchesin M and Sabeti M, Assessing the Efficiency of Different Control Strategies for the Coronavirus (COVID-19) Epidemic. arXiv 2020, 2004.03539
42. Sardar T, Nadim SS, Rana S, Chattopadhyay J. Assessment of lockdown effect in some states and overall India: A predictive mathematical study on COVID-19 outbreak. Chaos Solitons Fractals. 2020;139:110078. doi:10.1016/j.chaos.2020.110078
43. Aràndiga F, Baeza A, Cordero-Carrión I, Donat R, Martí MC, Mulet P, Yáñez DF. A spatial-temporal model for the evolution of the COVID-19 pandemic in Spain including mobility. Mathematics 2020;8(10):1677. https://doi.org/10.3390/math8101677
44. Tariq A, Undurraga EA, Laborde CC, Vogt-Geisse K, Luo R, Rothenberg R, Chowell G. Transmission dynamics and control of COVID-19 in Chile, March-October, 2020. PLoS Negl Trop Dis. 2021;15(1):e0009070. https://doi.org/10.1371/journal.pntd.0009070
45. Tariq A et.al., Transmission dynamics and forecasts of the COVID-19 pandemic in Mexico, March 20-November 11, 2020 MedRxiv 2021.01.11.21249561; doi: https://doi.org/10.1101/2021.01.11.21249561
46. Sattenspiel L, Dietz K. A structured epidemic model incorporating geographic mobility among regions. Math Biosci. 1995;128:71–91.
47. Arino J, Davis JR, Hartley D, Jordan R, Miller JM, van den Driessche P. A multi-species epidemic model with spatial dynamics. Math Medicine Biol. 2005;22(2):129–42.
48. van den Driessche P. Deterministic compartmental models: extensions of basic models. In: Brauer F, van den Driessche P, Wu J, editors. Mathematical epidemiology. Berlin: Springer; 2008. p. 147–57.

49. van den Driessche P. Spatial structure: patch models. In: Brauer F, van den Driessche P, Wu J, editors. Mathematical epidemiology. Berlin: Springer; 2008. p. 179–89.
50. Arino J. Diseases in metapopulations. In Ma Z, Zhou Y, Wu J, editors. Modeling and dynamics of infectious diseases. Beijing: Higher Education Press; 2009. p. 64–122.
51. Bürger R, Chowell G, Mulet P, Villada LM. Modelling the spatial-temporal progression of the 2009 A/H1N1 influenza pandemic in Chile. Math Biosci Eng. 2016;13:43–65.
52. van den Driessche P, Watmough J. Reproduction numbers and sub-threshold endemic equilibria for compartmental models of disease transmission. Math Biosci. 2002;180:29–48.
53. Wikipedia Commons, map of Chile, https://commons.wikimedia.org/wiki/File:Mapa-chile.svg, accessed February 7, 2021.
54. http://www.censo2017.cl/descargas/home/sintesis-de-resultados-censo2017.pdf, accessed February 7, 2021.
55. Government of Chile, https://www.gob.cl/coronavirus/cifrasoficiales/#reportes. Official COVID-19 website, accessed February 16, 2021.
56. Ministery of Science, Technology, Knowledge and Innovation of Chile, http://www.minciencia.gob.cl/covid19. Website of the official database for COVID-19 research; accessed February 16, 2021.
57. Chowell G, Fenimore PW, Castillo-Garsow MA, Castillo-Chavez C. SARS outbreaks in Ontario, Hong Kong and Singapore: the role of diagnosis and isolation as a control mechanism. J Theor Biol. 2003 Sep 7;224(1):1-8. doi: 10.1016/s0022-5193(03)00228-5. PMID: 12900200; PMCID: PMC7134599
58. Zou, L., et al., SARS-CoV-2 Viral Load in Upper Respiratory Specimens of Infected Patients. New England Journal of Medicine, 2020.
59. You C., et al., Estimation of the time-varying reproduction number of COVID-19 outbreak in China, International Journal of Hygiene and Environmental Health, 2020, 113555, ISSN 1438-4639, https://doi.org/10.1016/j.ijheh.2020.113555.
60. Linton, N.M.; Kobayashi, T.; Yang, Y.; Hayashi, K.; Akhmetzhanov, A.R.; Jung, S.-m.; Yuan, B.; Kinoshita, R.; Nishiura, H. Incubation Period and Other Epidemiological Characteristics of 2019 Novel Coronavirus Infections with Right Truncation: A Statistical Analysis of Publicly Available Case Data. J. Clin. Med. 2020, 9, 538. https://doi.org/10.3390/jcm9020538
61. Nishiura H., et al., Estimation of the asymptomatic ratio of novel coronavirus infections (COVID-19), Int J Inf Dis. 2020;94:154–5. https://doi.org/10.1016/j.ijid.2020.03.020
62. Mizumoto K, Kagaya K, Zarebski A, Chowell G. Estimating the asymptomatic proportion of coronavirus disease 2019 (COVID-19) cases on board the Diamond Princess cruise ship, Yokohama, Japan, Euro Surveill. 2020. https://doi.org/10.2807/1560-7917.ES.2020.25.10.2000180
63. Sun H, Qiu Y, Yan H, Huang Y, Zhu Y, Gu J, and Chen S. Tracking Reproductivity of COVID-19 Epidemic in China with Varying Coefficient SIR Model, Journal of Dara Science 2021. doi:10.6339/JDS.20200718(3).0010
64. Zhou C, Evaluating new evidence in the early dynamics of the novel coronavirus COVID-19 outbreak in Wuhan, China with real time domestic traffic and potential asymptomatic transmissions, medRxiv 2020. doi: https://doi.org/10.1101/2020.02.15.20023440
65. China CDC, The Epidemiological Characteristics of an Outbreak of 2019 Novel Coronavirus Diseases (COVID-19) −China, 2020, T.N.C.P.E.R.E. Team, Editor. 2020: China CDC Weekly.
66. Confinamiento por la pandemia de COVID-19 en Chile. [2/11/2021]; Available from: https://es.wikipedia.org/wiki/Confinamiento_por_la_pandemia_de_COVID19_en_Chile
67. McKinley T, Cook AR, Deardon R. Inference in epidemic models without likelihoods. Int J Biostat. 2009;5(1):24. https://doi.org/10.2202/1557-4679.1171
68. Zhao Z, Li X, Liu F, Zhu G, Ma C, Wang L. Prediction of the COVID-19 spread in African countries and implications for prevention and control: A case study in South Africa, Egypt, Algeria, Nigeria, Senegal and Kenya. Science Total Env. 2020;729:138959. https://doi.org/10.1016/j.scitotenv.2020.138959
69. Zhan C, Zheng Y, Lai Z, Hao T, Li B. Identifying epidemic spreading dynamics of COVID-19 by pseudocoevolutionary simulated annealing optimizers. Neural Comput & Applic 2020; https://doi.org/10.1007/s00521-020-05285-9
70. Chowell G. Fitting dynamic models to epidemic outbreaks with quantified uncertainty: A primer for parameter uncertainty, identifiability, and forecast. Infect Disease Model. 2017;2:379–398.

71. Roosa K, Chowell G. Assessing parameter identifiability in compartmental dynamic models using a computational approach: application to infectious disease transmission models. Theor Biol Med Model. 2019;16:1.
72. Chitnis N, Hyman JM, Cushing JM. Determining omportant parameters in the spread of malaria through the sensitivity analysis of a mathematical model. Bull Math Biol. 2008;70:1272–96. DOI 10.1007/s11538-008-9299-0